

Microbiome and metabolome alterations in Nrf2 knockout mice with induced gut inflammation and fed with phenethyl isothiocyanate and cranberry enriched diets

Ran Yin^{1*}, Davit Sargsyan^{1,2,3*}, Renyi Wu^{1*}, Rasika Hudlikar¹, Shanyi Li¹, Hsiao-Chen Kuo^{1,2}, Md Shahid Sarwar^{1,2}, Yuyin Zhou⁴, Zhan Gao⁵, Amy Howell⁶, Chi Chen⁴, Martin J. Blaser⁵ and Ah-Ng Kong^{1*}

¹Department of Pharmaceutics, Ernest Mario School of Pharmacy, Rutgers, The State University of New Jersey, Piscataway, NJ 08854, USA

²Graduate Program in Pharmaceutical Science, Ernest Mario School of Pharmacy, Rutgers, The State University of New Jersey, Piscataway, NJ 08854, USA

³Johnson & Johnson, Translational Medicine and Early Development Statistics, Raritan, NJ, USA

⁴Department of Food Science and Nutrition, University of Minnesota, ~~1354~~ St. Paul, MN 55108, USA.

⁵Center for Advanced Biotechnology and Medicine, Rutgers, The State University of New Jersey, Piscataway, NJ, 08854, USA

⁶Rutgers University Marucci Center for Blueberry Cranberry Research, 125A Lake Oswego Road, Chatsworth, NJ 08019

* Equal contribution

Correspondence

Professor Ah-Ng Tony Tong Kong

Rutgers, the State University of New Jersey

Ernest Mario School of Pharmacy, Room 228

160 Frelinghuysen Road, Piscataway, NJ 08854

Phone: +1-848-445-6369/8

Email: kongt@pharmacy.rutgers.edu

Abbreviations

ARE - antioxidant response element
DSS – dextran sulfate sodium
NRF2- NF-E2-related factor 2
OTU – operational taxonomic unit
PCA – principal components analysis
PEITC - phenethyl isothiocyanate
qPCR - quantitative polymerase chain reaction

Keywords: microbiome, Nrf2, PEITC, cranberry, DSS

Abstract

Scope

Cranberries are enriched with antioxidants and can help prevent bacterial infections, while phenethyl isothiocyanate (PEITC) found in cruciferous vegetables has anti-cancer and anti-inflammatory properties. Incorporating these into diet may have potential health benefits for human gut. Interactions of microbiome and metabolites with the host's cells play crucial roles in maintaining gastrointestinal (GI) tract balance.

Methods and results

In this study, we focused on the alteration of gut microbiomes and metabolomes by cranberry and PEITC enriched diets in wild-type (WT) and Nrf2 knockout (KO) mice, and the diets' potential in reducing the risk of inflammation. Nrf2 KO mice had higher alpha diversity compared to WT. Cranberry and PEITC limited the inflammatory effect of dextran sulfate sodium (DSS) and increased the diversity of ~~mice~~ gut microbiota. DSS challenge altered the production of several metabolites while PEITC and cranberry feeding reversed the changes. The enriched diets modulated the metabolic responses to induced inflammation likely via microbial composition alterations. Nrf2 KO mice had lower levels of short-chain fatty acids (SCFA) and amino acids such as glutamate, phenylalanine and ~~prolin~~, and higher levels of secondary bile acids such as DCA, LCA and MCA compared to WT mice

Conclusions

We observed higher microbiome richness and diversity in the Nrf2 KO mice compared to WT. The results also suggest that PEITC and cranberry-infused diets had protective effect on the hosts' microbiome richness and diversity and increased the production of microbial metabolites. Additionally, the dietary supplements showed the reversal of the negative effect of DSS-induced inflammation on the balance of Firmicutes and Bacteroidetes, the two major phylum in the hosts' intestines. Taken together, our current study indicates that the phenotypic expression of Nrf2 impacted the microbiota and metabolic reprogramming induced by DSS-mediated inflammation and dietary feeding of cranberry and PEITC which are positively associated with the health of human gut.

1. Introduction

Human and animal health can be affected by microorganisms including bacteria, archaea and fungi which are distributed in large quantities on surfaces throughout their bodies (1). The role of gut bacteria is especially noted for their potential beneficial effects in metabolizing essential nutrients, providing energy and enhancing immune system (2, 3, 4). For example, gut bacteria *Butyricoccus Pullicaecorum* and ~~*Butyricoccus Pullicaecorum*~~ produce butyrate, an essential metabolite for human GI homeostasis and disease prevention (5). Lactobacillus strains are involved in essential vitamins metabolism (6) and human sleep quality improvement (7). Yet another group of bacterial strains, bifidobacterium might be able to influence human emotions like depression, reduce painful feeling, and alter brain activity during stress (8, 9, 10, 11, 12). Numerous studies have been conducted to explore gut microbiota composition responding to specific conditions such as high fat or high fiber diet, or inflammatory bowel disease (13, 14, 15),

16, 17, 18, 19, 20, 21). In addition, research suggest that host's genotype may influence the human gut microbiota, especially the infant period (22, 23). The combination of host genotype, gut microbiota and postnatal factors such as antibiotic usage, dietary pattern and environmental microbes shows significant influence on human gut development and homeostasis (24, 25). Hence, the underlying mechanism of such microbiota-host crosstalk is crucial but remains poorly understood.

Cranberry have been consumed historically by Native Americans as food and medicine (26). Today, cranberry is widely consumed as fresh and dried fruit, juice and sauce. The berries are known for their high content of proanthocyanidins, flavonoids and other organic acids (27, 28). Cranberry consumption have been associated with reduced risk of urinary tract infections (29, 30) and inflammation (31), and improved cardiovascular health (32).

Phenethyl isothiocyanate (PEITC) is a member of the isothiocyanate family of compounds which are formed when glucosinolates, a class of sulfur-containing compounds found in cruciferous vegetables, are hydrolyzed by enzymes (33, 34). PEITC has been found to have a wide range of biological activities including anticancer, anti-inflammatory, and antioxidant effects (35, 36).

Gut microbiome composition determines how efficiently food is processed into metabolites such as amino acids, bile acids and short-chain fatty acids. In our study we used C57BL/6J wild type (WT) and Nrf2 gene knockout (KO) mice to test diets to which either cranberry or PEITC were added since both have been shown to boost the production of these metabolites. Possible health benefits of these food additives include cancer prevention and activation of Nrf2 pathway, a master regulator of oxidative stress and inflammation. The aim of this study was to understand the mechanisms by which cranberry and PEITC can influence the gut microbiome and microbial metabolite production, and further improve the gut health via reducing inflammation and achieving homeostasis.

2. Materials and Methods

2.1 Animals and Study Design

C57BL/6J WT mice were purchased from Jackson Laboratory (Bar Harbor, ME). C57BL/6J Nrf2 KO mice have been maintained in our laboratory since 2005 (37, 38). Mice were kept in a controlled temperature (20–22°C) and humidity (45–55%) environment under 12-hour light and dark cycles at the Rutgers Animal Facility. Food and water were provided ad libitum. The study was stacked into three experiments.

All mice were given a 2-week gut microbiota equalization period during which they were fed with AIN93M control diet (Research Diets, Inc. NJ).

In the first experiment (Exp01), 18 Nrf2 KO mice were randomized into 2 groups after the 2-week equalization period. One group continued receiving the control diet (AIN93M, regular grain diet) while the second group's diet was enhanced with 0.05% PEITC. In the second experiment (Exp2), 10 WT mice were randomized into either the control diet (AIN93M) or the PEITC-enhanced diet groups. In the third experiment (Exp03), additional cranberry-enriched diet was introduced (10% of feed by weight), and 20 mice were challenged with dextran sulfate

sodium (DSS) to induce gut inflammation. 2.5% DSS was dissolved in autoclaved water and made freshly weekly. Both, WT and Nrf2 KO genotypes were used, and the mice were randomized into one of four treatment groups (Naïve, DSS, DSS + PEITC, and DSS + Cranberry) within each genotype (Figure 1). Fecal samples were collected freshly snap frozen in liquid nitrogen and stored at -80°C for 16S ribosomal RNA (rRNA) sequencing and microbial metabolites analysis. Fecal samples for 16S sequencing were collected at weeks 1 and 5 in Exp01, weeks 0 and 4 in Exp02, and weeks 0, 1 and 8 in Exp03. Additional samples were collected from all mice for metabolomics analysis at weeks 2 and 6 in Exp03. Since the fecal sample collection timing varied slightly between the experiments, it was realigned and labeled as baseline (end of the equalization period, i.e., Week 0), early (weeks 1 through 2) or late (weeks 4 through 8) timepoints.

All animal experiments were conducted under the animal protocol approved by the Institutional Animal Care and Use Committee (IACUC) of Rutgers University.

2.2 16S ribosomal RNA gene sequencing and analysis

Bacterial DNA were extracted using *PowerSoil DNA Isolation Kit* (QIAGEN). PCR amplification of the 16S rRNA genes were carried out using PCR primers specific for the V4 region (Supplemental Table 1) (39, 40, 41, 42, 43, 44, 45). Indexed amplicons were pooled and sequenced on *MiSeq* (Illumina) yielding at least 8,000 300 base pair (bp) pair-ended reads. Microbial operational taxonomic units (OTUs) and their taxonomic assignments were analyzed using Quantitative Insights Into Microbial Ecology (QIIME2) bioinformatic pipeline (46, 47) and Divisive Amplicon Denoising Algorithm 2 (DADA2 version 1.16) *R* package (48).

QIIME2 mapped reference at 97% similarity against representative sequences of 97% OTU in SILVA, a high quality rRNA database (49), followed by chimeric sequences removal from subsequent analyses (50). Principle coordinates analysis (PCoA) on the unweighted unique fraction metric (UniFrac) was performed to visualize similarity of microbial communities of the samples.

DADA2 pipeline was used to process *FastQ* sequence data files containing pair-ended reads with average length of 300 base pairs (bp) into a high-resolution OTU table (i.e., amplicon sequencing variants). The reads were sorted, and quality scores examined, resulting in truncation of forward reads to 280 bp and reverse reads to 220 bp based on the quality score profiles. The reads were then merged and aggregated. Additionally, chimeric OTUs were identified and removed. Taxonomy was assigned to the OTUs by exact matching (100% identity) to SILVA reference database.

2.3 Microbial metabolites analysis

The concentrations of microbial metabolites (free amino acids, bile acids and SCFA) were quantified in fecal samples collected at weeks 2 and 6 using liquid chromatography mass spectrometry (LC-MS)-based targeted ~~and untargeted~~ analysis.

2.4 Statistical Analyses

Alpha diversity was assessed using Shannon's index at OTU level. The index is equal to zero when there is exactly one class (a single OTU) present in a sample. Larger values of the index



indicate greater number of and more evenly distributed OTUs, with the highest value of the index reaching $\ln(k)$ with k equally distributed OTUs. The estimates were presented as means +/- standard error of the means (SEM).

Multivariable analysis of variance (ANOVA) using genotype, diet and timepoints was performed followed by multiple comparison with false discovery rate (FDR) adjustment for the p-values.

Bacterial composition at different taxonomic levels was explored using principal components analysis (PCA) and visualized as biplots. PCA is a linear transformation that projects the data from the original n -dimensional, correlated space (here, each taxonomic unit was viewed as a dimension) onto a new, orthogonal n -dimensional space such that the first principal component (PC1) is in the direction that explains most of variability in the data, the second (PC2) - the second most and orthogonal to PC1, and so on. The samples were then plotted against 2 principal components (e.g., PC1 and PC2) and color-coded to check for group separation. Biplot is an extension of PCA plot that simultaneously display the labeled samples in two principal components' space as well as the direction and the magnitude of the original axes (i.e., individual taxonomic units). Multinomial regression on class (group labeling corresponding to taxonomic units) vs. principal components was performed to statistically assess the predictive power of PCA on class separation.

Metabolites' quantities were presented as heatmaps. ANOVA was used to test for group mean differences for each metabolite individually and presented as boxplots with bars and stars indicating statistically significantly different groups.

3 Results

3.1 Data acquisition

Sequencing depth varied between 30,008 and 422,283 reads per sample (Supplemental Figure 1). Over 94% of OTUs were identified as bacterial. OTUs mapped to *Eukaryota* and *Archaea* Kingdoms, as well as OTUs that could not be mapped to a Kingdom, were removed. In total, 10,197 (94.78% of total OTUs), 7,994 (98.34%) and 7,558 (96.07%) bacterial OTUs were identified in the 3 experiments respectively (Table 1).

Additionally, bacterial OTUs belonging to phylum *Cyanobacteria* were removed as contamination from diet. Finally, OTUs not mapped to any bacterial phylum were removed, and the remaining OTUs analyzed.

3.2 Diet, genotype and inflammation affect bacterial community richness and diversity
 Nrf2 is a master regulator of anti-oxidative stress and anti-inflammatory responses to external and internal stimuli (51, 52, 53, 54, 55). The impact of Nrf2 was examined by comparing the Nrf2 knockout (KO; -/-) mice vs. the control (WT) at different conditions (diet, DSS challenge, and aging). Alpha diversity analysis of the bacterial OTUs was conducted using Shannon index (Figure 2A).

Mixed-effects regression analysis showed that the alpha diversity was higher in Nrf2 KO compared to the WT genotypes ($p\text{-value} < 0.01$), went up as the study progressed (both, the p-values for the early and the late timepoints vs. the baseline < 0.01), and was lower in the DSS+PEITC and DSS+Cranberry diet groups compared to the group that was not challenged with DSS (both p-values < 0.01).

However, Shannon index (as well as other indices measuring inequalities in the samples) is biased by the sample's sequencing depth. Specifically, deeper sequencing results in identification of more, rare OTUs, therefore inflating the index (Supplemental Figure 2A). To remediate for this effect, a sensitivity analysis was conducted by, first, adding 1 to all counts in the combined OTU table. Even though the zeros in the table could represent either complete absence of an OTU from a sample or very low abundance, the zeros were treated similarly here. This remediation removed the Shannon index/sequencing depth correlation (Supplemental Figure 2B). After repeating the analysis on the corrected Shannon index, genotype differences remained statistically significant (higher alpha diversity in the Nrf2 KO group compared to WT, $p\text{-value} = 0.02$) but aging effect disappeared and only the DSS+AIN93M group's alpha diversity remained significantly lower compared to the group not challenged with DSS ($p\text{-value} < 0.01$). These results suggest that PEITC and cranberry-rich diets had protective effect on the hosts' microbiome diversity. The averages of the corrected Shannon indices are presented in Figure 2B.

3.2 Principal components analysis reveal association of microbiome composition with diet and genotype

OTU counts were aggregated at the ***Phylum*** level. In total, 22 phyla were identified, top 10 of which accounted for $>99.96\%$ of all hits. Since deeper sequencing increases chances of identifying rare organisms (Supplemental Figure 3), and the samples varied greatly by sequencing depth (Supplemental Figure 1), rare *phylum* were not included in the downstream analysis. PCA was conducted on the combined data from the 3 experiments, but scores and loadings were graphed in separate panels by genotype and experiment to highlight the differences (Figure 4). The biplot showed large between-experiment variability, specifically, higher relative abundance of *Bacteroidetes*, and lower relative abundance of *Verrucomicrobia* in the first two experiments (Exp01 and Exp02) compared to the third one (Exp03). Relative abundances of *Firmicutes* and *Actinobacteria* were higher in the WT DSS-treated mice in the Exp03 compared to all other groups, while *Epsilonbacteraeota* were more abundant in all Nrf2 KO and WT control (AIN93M) groups compared to the rest. Additionally, DSS+PEITC group samples showed trend reversal from the positive control (DSS+AIN93M) group in WT, suggesting protective effect of PEITC on microbiome of DSS-treated mice.

The top 10 most abundant *Phylum* were used for the PCA. The analysis revealed strong diet effect on the microbial composition. Specifically, relative abundance of *Firmicutes* and *Verrucomicrobia* increased while relative abundance of *Proteobacteria*, *Deferribacteres* and *Epsilonbacteraeota* decreased in all WT DSS-treated groups compared to the control (AIN93M). To remove study effect while examining Nrf2 KO effect, Exp03 data was separated and reanalyzed (Figure 5).

Class-level aggregation yield 31 classes, with top 17 adding up to >99.99% of the total hits. The PCA showed strong negative effect of Nrf2 KO on *Bacilli* class (phylum (p.) *Firmicutes*) that was consistent in all 3 experiments (Figure 6). Separate analysis of Exp03 data identified 18 out of the 31 classes, with 2 of them at a very low level, hence, only 16 classes were used in this analysis. The biplot (Figure 7) showed clear separation by genotype. Relative abundance of *Clostridia* (p. *Firmicutes*) was higher while *Betaproteobacteria*, *Epsilonproteobacteria* and *Deltaproteobacteria* (p. *Proteobacteria*), as well as *Campylobacter* (p. *Epsilonbacteraeota*), *Brachyspirae* (p. *Spirochaetes*), and *Deferrribacteres* (p. *Deferrribacteres*) were lower in the all three DSS-treated groups. *Verrucomicrobiae* (p. *Verrucomicrobia*) and *Gammaproteobacteria* (p. *Proteobacteria*) had higher relative abundance in the DSS+AIN93M and DSS+Cranberry groups.

3.3 Firmicutes/Bacteroidetes ratio

Firmicutes to Bacteroidetes ratio (F/B) have been linked to biological activity including aging (56) and body mass index change (57) and maintaining intestinal homeostasis. Increased F/B ratio was associated with obesity while the ratio decreased was correlated positively with inflammatory bowel disease (58). In this study, the F/B ratios were calculated within each sample and compared across the experiments, genotype, diet and timepoints (Figures 8). Samples from Exp01 and Exp02 contained equal or lower abundance of Firmicutes compared to Bacteroidetes but the F/B ratios in the WT mice samples were higher than in the Nrf2 KO samples in all 3 experiments. Formal analysis using a mixed-effects linear regression models was conducted on Exp03. A model with no interaction terms showed significant decrease of F/B ratio in DSS+PEITC and DSS+Cranberry groups ($\log_2[F/b] = -0.51$ and -0.46 , and p-values <0.01 and $=0.01$, respectively) as well as decrease in the Nrf2 KO group compared to WT ($\log_2[F/B] = -1.02$, p-value <0.01). The control diet group (AIN93M, no DSS challenge) average F/B ratio difference with the DSS control (DSS+AIN93M) as well as difference between early or late vs. timepoints vs. baseline were not statistically significant. Results from a model containing an interaction term for the genotype and diet confirmed significant association of F/B ratio with genotype ($\log_2[F/B] = -1.40$, p-value <0.01), as well as with PEITC and Cranberry diets ($\log_2[F/b] = -0.60$ and -0.71 , respectively, with both p-values <0.01). Additionally, the F/B ratio of the AIN93M group was significantly lower than the DSS+ AIN93M ($\log_2[F/B] = -1.40$, p-value <0.01). These results suggest that PEITC and Cranberry supplements to regular grain diet reversed the effect of DSS challenge on the balance of Firmicutes and Bacteroidetes in the hosts' intestines.

3.4 Linear Discriminant Analysis of aging and dietary effects

To further examine the potential differences of the microbiota between the control (AIN93M) and the PEITC diets, a parallel analysis in QIIME2 was conducted using Linear discriminant analysis Effect Size (LEfSe).

Firstly, the potential aging effect on the microbiota was examined by comparing the control samples at baseline (shown in Figure 9 in red) with the early (Week 1) and late (Week 4) timepoints (shown in green). Taxa with relative abundance $\geq 0.1\%$ present in at least one specimen were included. In addition, the cladograms showing the phylogenetic distribution of

the microbial lineages associated with different time points, using lineages with Linear Discriminant Analysis (LDA) score ≥ 2.0 were displayed. *Bacteroidetes Prevotella*, *Bacteroidetes Parabacteroides*, *Bacteroidetes*, and *Bacteroidetes S24_7* relative abundance decreased, while *Bacteroidetes Bacteroidales*, *Firmicutes Clostridiales*, *Firmicutes Oscillospira*, *Proteobacteria Desulfovibrionaceae*, and *Tenericutes Anaeroplasma* increased over time.

Next, the impact of PEITC-supplemented diet was examined. Figures 10 show the impact of PEITC diet by comparing the microbiota for control diet at baseline (Week 0, shown in red) and at the later timepoints (Weeks 1 or 4, shown in green). Relative abundance of *Firmicutes Ruminococcus* significantly increased and *Bacteroidetes S24_7* significantly decreased at both at the later time points compared to baseline. Some bacteria were uniquely correlated with diet. *Bacteroidetes Odoribacter*, *Tenericutes Mycoplasmataceae* and *Proteobacteria Desulfovibrionaceae* significantly higher relative abundance in the control (AIN93M) group while *Firmicutes Clostridiales*, *Firmicutes Ruminococcus* and *Acidobacteria Ellin 6075* were found in significantly higher abundance in the PEITC group.

3.5 PEITC and cranberry feeding partially reverse the DSS-induced changes in fecal metabolome

Metabolomics profiles of DSS, DSS + PEITC, and DSS + Cranberry treatment group fecal samples collected at weeks 2 and 6 were analyzed and the concentrations of free amino acids, bile acids and SCFA were quantified (Exp03 only).

Principal components analysis showed that overall levels of all but one (taurine) amino acids were elevated in the Cranberry diet group (Figure 11A). However, for bile acids genotype rather than diet played a bigger role, with higher production of all bile acids in the Nrf KO and especially increase of LCA, DCA, MCA, CDCA, GDCA and GCDCA driving the separation between the two genotypes (Figure 11B).

Multinomial regression models were fitted to classify sample treatment and diet or genotype with principal components as predictors. The model with the first 3 principal components accurately classified 29 out of 48 samples (60.4%) by treatment/diet and the predictive power increased slow by adding more PC (Table 2). However, the model for genotype correctly classified 34 out of 48 samples (70.8%) with just the first principal component (Table 3) suggesting stronger separation of the samples by genotype.

Examination of the metabolites individually showed that DSS treatment altered the production of several of them while PEITC and cranberry feeding reversed the changes (Figure 12A). For example, DSS decreased the concentrations of many amino acids such as glutamate, phenylalanine, and proline, but PEITC and cranberry cotreatments prevented these decreases (Figure 12B-D). Furthermore, PEITC and cranberry cotreatments reversed the DSS-induced increases of ~~secondary~~ bile acids, mainly deoxycholic acid (DCA), lithocholic acid (LCA), and muricholic acid (MCA) (Figure 12E-G). In contrast, PEITC and cranberry cotreatments had limited effects on the DSS-induced changes in SCFA (Figure 12H-J). Overall, these data indicated that PEITC and cranberry (rich in anthocyanins) are capable of modulating the

metabolic responses to DSS treatment in the colorectal tract, potentially through their effects on the microbiome.

In addition, the concentrations of fecal metabolites were compared between WT and Nrf2 KO mice. Interestingly, compared to WT, Nrf2 KO mice had lower levels of amino acids (shown by glutamate, phenylalanine, and proline) and SCFA, and higher levels of ~~secondary~~ bile acids (shown by DCA, LCA, and MCA) than WT mice (Figure 13A-I), which were similar to the metabolite profile of DSS-treated WT mice.

4 Discussion

Systematic studies of gut microbiome regulators have shown that diet ~~and host genotype~~ play important role in ~~host-diet-microbiome interaction~~. For instance, a rapid and consistent dietary response to low fat/high plant polysaccharide, and high fat/sugar diet on gene deficient mice has been reported to co-occur with significant increase of relative abundance of *Firmicutes* (*Clostridiales*, *Lactobacillales*, *Turicibacterales*) and *Verrucomicrobia* (*Verrucomicrobiales*). In contrast, *Bacteroidetes* (*Bacteroidales*) significantly decreased in high fat/sugar diet group. Additionally, *Clostridiales* and *Bacteroidales* significantly altered composition of bacterial orders during the dietary shift between low fat/high plant polysaccharide diet and high fat/sugar diet. Utilizing gnotobiotic mouse model with transplantation of healthy human fecal sample, the low fat/high plant polysaccharide diet decreased the relative abundance of *Firmicutes Erysipelotrichi*, *Firmicutes Bacilli*, and increased the relative abundance of *Bacteroidetes Bacteroidetes* compared with high fat/sugar Western diet. Twenty-eight healthy subjects were given 60 g of whole grain barley, brown rice or equal mixture of two ingredients every day for 4 weeks (59). All three whole grain diets significantly increased the gut bacterial diversity (Shannon's and Simpson's indices), and the proportion of phylum *Firmicutes*, while decreases the proportion of phylum *Bacteroidetes*. At the individual level, genus *Bacteroides* were significantly decreased by whole barley and brown rice mix diet but were not affected by either of the single ingredient diet. In addition, genus *Roseburia*, *Bifidobacterium*, *Dialister* and *Odoribacter* were significantly altered only by whole grain barley diet, and genus *Blautia* by both, mix diet and whole grain barley diet. 

Host genotype may also influence the human gut microbiota, ~~although opinions regarding its contribution diverge due to the potential confounding factors such as the diet. Simplified animal model~~ using the same diet and living environment can ~~help~~ reveal the potential relationship between genotype and gut microbiota ~~and helps remove some of the doubts~~. Results from a ~~mice~~ study conducted in 2011 (60) that used automated ribosomal intergenic spacer analysis and length-heterogeneity polymerase chain reaction (L-H PCR) (61) suggested that the observed gut microbiota alterations were genotype-dependent as all animals were housed at the same facility and given the same diet. Higher dissimilarities between genotypes than sexes were observed suggesting that genotype is a stronger factor than gender in regulating gut microbiota. Another evidence of gut microbiota determined by genotype comes from a genetic defect of toll-like receptor 2 (TLR2)-deficient mouse study (62). The genus level of *Helicobacter* was significantly elevated in TLR2 knock-out mice compared to the wild type. Moreover, some genetic defect such as NOD2 and ATG16L1 were linked to inflammatory bowel diseases and suggested the

host-microbiota interaction by shifting bacterial composition including relative abundance of *Actinobacteria*, *Firmicutes*, and *Proteobacteria*.

Gut bacteria have been appreciated for many years with its potential beneficial effects in metabolizing essential nutrients, providing energy and enhancing immune system (2, 3, 4). For instance, gut bacteria *Butyricicoccus Pullicaecorum* and *Butyricicoccus Pullicaecorum* produce butyrate, an essential metabolite for human homeostasis and disease prevention (5) while *Lactobacillus* strains are involved in essential vitamins metabolism (6). The current study demonstrated that host genotype and diet may alter gut microbiota. Both bacterial diversity and individual bacterial strains changed significantly based on different genotype and diet, and Nrf2 KO genotype showed stronger effects on the bacterial diversity than diet. *Firmicutes*, *Bacteroidetes* and *Proteobacteria*, the most abundant bacterial phyla, have been altered by both, diet and Nrf2 KO. Individual bacteria at different taxonomic levels showed a pattern of being consistently affected by both, genotype and diet. For instance, *Firmicutes Ruminococcus* was observed to be in higher relative abundance in the PEITC-supplemented groups and in Nrf2 KO mice.

Ruminococcus are anaerobic, gram-positive bacteria and belong to the phylum of *Firmicutes*. So far, eleven *Ruminococcus* species have been identified and fall into bacterial family *Ruminococcaceae* and *Lachnospiraceae* (63, 64). Previous studies showed that *Ruminococcus* degraded and fermented cellulosic biomass into short-chain fatty acid (SCFA) for herbivorous ruminants (65, 66, 67). *Ruminococcus Torques* was reported to be abundant in the irritable bowel syndrome subjects in a placebo control double blind study (68). Multiple probiotic interventions were able to reduce *Ruminococcus Torques* abundance significantly based on results obtained from quantitative real-time polymerase chain reaction (qPCR), suggesting that *Ruminococcus Torques* may be used as biomarker in evaluating probiotic activity. As a part of normal flora in gastrointestinal tract, another *Ruminococcus* species, *Gnavus* showed to be in high abundance in the IBD patients, with increased level of oxidative stress in the gut (69), potentially caused by cytokine production such as TNF-a (70). *Firmicutes* has also been reported to be overpopulated in infants who developed respiratory and skin allergic diseases (71). Mice orally garaged by purified *Ruminococcus Gnavus* also developed airway inflammation by cytokine secretion such as interleukin 25, 33 and others. In this study, we observed a significant increase in the abundance of *Firmicutes Ruminoccus* in fecal samples at the late but not at the early timepoints irrespective of diet and genotype. Accumulation of harmful inflammatory bacteria in the guts is considered has been linked to aging. However, we found that the increased level of *Firmicutes Ruminoccus* was mainly associated with Nrf2 KO suggesting that Nrf2 KO accelerates the increase of *Firmicutes Ruminoccus*'s relative abundance. This suggests that Nrf2 might play an important role in regulating the gut microbiota profile and suppress pathogenic species such as *Firmicutes Ruminoccus* as the animal age.

Interestingly, we also observed that the phylum *Ruminoccus* were elevated at the early timepoint in the PEITC groups. *Bacteroidetes Rikenella* was also found significantly elevated in Nrf2 KO groups, suggesting that it may correlate with gut diseases (72, 73, 74, 75). Overall, genetic KO

(mutation) has a strong impact on the host microbiota profile over time and should be considered as a biomarker when developing probiotic or microbiota intervention therapy in the future.

In this study, we conclude that *mice* genotype is strongly associated with gut microbiome richness and diversity and compositional changes. However, many more factors contribute to difference. Research has demonstrated that cage and internal individual effects are contributing up to 32% and 46% of gut microbiota variability, respectively (76). Several methods are used to eliminate the background noise that include feeding the animals with a control diet for several weeks to equalize microbiomes at baseline or using gnotobiotic (germ-free) mice implanted with homogenized fecal samples (77, 78, 79). In this study, we employed the former, but it still produced moderate level of variability at the baseline. However, gnotobiotic models are not without complications as they require germ-free facilities and the animals' immune system may be affected by the lack of microbiome at the early stages of their lives. A middle ground can be reached by pretreating the animals with wide-spectrum antibiotics and providing them with high fiber content food before implanting them with homogenized fecal samples (80).

5 Acknowledgment



6 Conflict of Interests

The authors declare no conflicts of interest.

7 Autor Contribution

All authors contributed significantly to this manuscript.

8 References

1. Dethlefsen L, McFall-Ngai M, Relman DA. An ecological and evolutionary perspective on human-microbe mutualism and disease. *Nature*. 2007;449(7164):811-8.
2. Ramakrishna BS. Role of the gut microbiota in human nutrition and metabolism. *J Gastroen Hepatol*. 2013;28:9-17.
3. Rowland I, Gibson G, Heinken A, Scott K, Swann J, Thiele I, et al. Gut microbiota functions: metabolism of nutrients and other food components. *Eur J Nutr*. 2018;57(1):1-24.
4. Maslowski KM, Mackay CR. Diet, gut microbiota and immune responses. *Nat Immunol*. 2011;12(1):5-9.
5. Geirnaert A, Calatayud M, Grootaert C, Laukens D, Devriese S, Smagghe G, et al. Butyrate-producing bacteria supplemented in vitro to Crohn's disease patient microbiota increased butyrate production and enhanced intestinal epithelial barrier integrity. *Sci Rep-Uk*. 2017;7.
6. LeBlanc JG, Milani C, de Giori GS, Sesma F, van Sinderen D, Ventura M. Bacteria as vitamin suppliers to their host: a gut microbiota perspective. *Curr Opin Biotech*. 2013;24(2):160-8.
7. Aizawa E, Tsuji H, Asahara T, Takahashi T, Teraishi T, Yoshida S, et al. Bifidobacterium and Lactobacillus Counts in the Gut Microbiota of Patients With Bipolar Disorder and Healthy Controls. *Front Psychiatry*. 2018;9:730.
8. Desbonnet L, Garrett L, Clarke G, Kiely B, Cryan JF, Dinan TG. Effects of the Probiotic *Bifidobacterium Infantis* in the Maternal Separation Model of Depression. *Neuroscience*. 2010;170(4):1179-88.
9. Schmidt C. Mental health: thinking from the gut. *Nature*. 2015;518(7540):S12-5.

10. Tillisch K, Labus JS, Ebrat B, Stains J, Naliboff BD, Guyonnet D, et al. Modulation of the Brain-Gut Axis After 4-Week Intervention With a Probiotic Fermented Dairy Product. *Gastroenterology*. 2012;142(5):S115-S.
11. Cryan JF, Dinan TG. Mind-altering microorganisms: the impact of the gut microbiota on brain and behaviour. *Nat Rev Neurosci*. 2012;13(10):701-12.
12. McKernan DP, Fitzgerald P, Dinan TG, Cryan JF. The probiotic *Bifidobacterium infantis* 35624 displays visceral antinociceptive effects in the rat. *Neurogastroent Motil*. 2010;22(9):1029-+.
13. Cani PD, Bibiloni R, Knauf C, Waget A, Neyrinck AM, Delzenne NM, et al. Changes in gut microbiota control metabolic endotoxemia-induced inflammation in high-fat diet-induced obesity and diabetes in mice. *Diabetes*. 2008;57(6):1470-81.
14. Kim KA, Gu W, Lee IA, Joh EH, Kim DH. High fat diet-induced gut microbiota exacerbates inflammation and obesity in mice via the TLR4 signaling pathway. *PLoS One*. 2012;7(10):e47713.
15. Daniel H, Gholami AM, Berry D, Desmarchelier C, Hahne H, Loh G, et al. High-fat diet alters gut microbiota physiology in mice. *ISME J*. 2014;8(2):295-308.
16. Shim JO. Gut microbiota in inflammatory bowel disease. *Pediatr Gastroenterol Hepatol Nutr*. 2013;16(1):17-21.
17. Eom T, Kim YS, Choi CH, Sadowsky MJ, Unno T. Current understanding of microbiota- and dietary-therapies for treating inflammatory bowel disease. *J Microbiol*. 2018;56(3):189-98.
18. Butel MJ. Probiotics, gut microbiota and health. *Med Maladies Infect*. 2014;44(1):1-8.
19. Sekirov I, Russell SL, Antunes LCM, Finlay BB. Gut Microbiota in Health and Disease. *Physiol Rev*. 2010;90(3):859-904.
20. Chen L, Liu B, Ren L, Du H, Fei C, Qian C, et al. High-fiber diet ameliorates gut microbiota, serum metabolism and emotional mood in type 2 diabetes patients. *Front Cell Infect Microbiol*. 2023;13:1069954.
21. Heinritz SN, Weiss E, Eklund M, Aumiller T, Louis S, Rings A, et al. Intestinal Microbiota and Microbial Metabolites Are Changed in a Pig Model Fed a High-Fat/Low-Fiber or a Low-Fat/High-Fiber Diet. *PLoS One*. 2016;11(4):e0154329.
22. Spor A, Koren O, Ley R. Unravelling the effects of the environment and host genotype on the gut microbiome. *Nat Rev Microbiol*. 2011;9(4):279-90.
23. Olivares M, Laparra JM, Sanz Y. Host genotype, intestinal microbiota and inflammatory disorders. *Br J Nutr*. 2013;109 Suppl 2:S76-80.
24. Carmody RN, Gerber GK, Luevano JM, Jr., Gatti DM, Somes L, Svenson KL, et al. Diet dominates host genotype in shaping the murine gut microbiota. *Cell Host Microbe*. 2015;17(1):72-84.
25. Ussar S, Griffin NW, Bezy O, Fujisaka S, Vienberg S, Softic S, et al. Interactions between Gut Microbiota, Host Genetics and Diet Modulate the Predisposition to Obesity and Metabolic Syndrome. *Cell Metab*. 2015;22(3):516-30.
26. Neto CC, Vinson JA. Cranberry. In: Benzie IFF, Wachtel-Galor S, editors. *Herbal Medicine: Biomolecular and Clinical Aspects*. 2nd ed. Boca Raton (FL)2011.
27. Feghali K, Feldman M, La VD, Santos J, Grenier D. Cranberry proanthocyanidins: natural weapons against periodontal diseases. *J Agric Food Chem*. 2012;60(23):5728-35.
28. Wang Y, Johnson-Cicalese J, Singh AP, Vorsa N. Characterization and quantification of flavonoids and organic acids over fruit development in American cranberry (*Vaccinium macrocarpon*) cultivars using HPLC and APCI-MS/MS. *Plant Sci*. 2017;262:91-102.
29. Jepson RG, Williams G, Craig JC. Cranberries for preventing urinary tract infections. *Cochrane Database Syst Rev*. 2012;10(10):CD001321.
30. Howell AB. Bioactive compounds in cranberries and their role in prevention of urinary tract infections. *Mol Nutr Food Res*. 2007;51(6):732-7.
31. Cai X, Han Y, Gu M, Song M, Wu X, Li Z, et al. Dietary cranberry suppressed colonic inflammation and alleviated gut microbiota dysbiosis in dextran sodium sulfate-treated mice. *Food Funct*. 2019;10(10):6331-41.

32. Reed J. Cranberry flavonoids, atherosclerosis and cardiovascular health. *Crit Rev Food Sci Nutr.* 2002;42(3 Suppl):301-16.
33. Johnson IT. Glucosinolates: bioavailability and importance to health. *Int J Vitam Nutr Res.* 2002;72(1):26-31.
34. Dayalan Naidu S, Suzuki T, Yamamoto M, Fahey JW, Dinkova-Kostova AT. Phenethyl Isothiocyanate, a Dual Activator of Transcription Factors NRF2 and HSF1. *Mol Nutr Food Res.* 2018;62(18):e1700908.
35. Gupta P, Wright SE, Kim SH, Srivastava SK. Phenethyl isothiocyanate: a comprehensive review of anti-cancer mechanisms. *Biochim Biophys Acta.* 2014;1846(2):405-24.
36. Keum YS, Owuor ED, Kim BR, Hu R, Kong AN. Involvement of Nrf2 and JNK1 in the activation of antioxidant responsive element (ARE) by chemopreventive agent phenethyl isothiocyanate (PEITC). *Pharm Res.* 2003;20(9):1351-6.
37. Shen G, Xu C, Hu R, Jain MR, Gopalkrishnan A, Nair S, et al. Modulation of nuclear factor E2-related factor 2-mediated gene expression in mice liver and small intestine by cancer chemopreventive agent curcumin. *Mol Cancer Ther.* 2006;5(1):39-51.
38. Lin W, Wu RT, Wu TY, Khor TO, Wang H, Kong AN. Sulforaphane suppressed LPS-induced inflammation in mouse peritoneal macrophages through Nrf2 dependent pathway. *Biochem Pharmacol.* 2008;76(8):967-73.
39. Apprill A, McNally S, Parsons R, Weber L. Minor revision to V4 region SSU rRNA 806R gene primer greatly increases detection of SAR11 bacterioplankton. *Aquat Microb Ecol.* 2015;75(2):129-37.
40. Caporaso JG, Lauber CL, Walters WA, Berg-Lyons D, Lozupone CA, Turnbaugh PJ, et al. Global patterns of 16S rRNA diversity at a depth of millions of sequences per sample. *P Natl Acad Sci USA.* 2011;108:4516-22.
41. Caporaso JG, Lauber CL, Walters WA, Berg-Lyons D, Huntley J, Fierer N, et al. Ultra-high-throughput microbial community analysis on the Illumina HiSeq and MiSeq platforms. *Isme J.* 2012;6(8):1621-4.
42. Minich JJ, Humphrey G, Benitez RAS, Sanders J, Swofford A, Allen EE, et al. High-Throughput Miniaturized 16S rRNA Amplicon Library Preparation Reduces Costs while Preserving Microbiome Integrity. *Msystems.* 2018;3(6).
43. Parada AE, Needham DM, Fuhrman JA. Every base matters: assessing small subunit rRNA primers for marine microbiomes with mock communities, time series and global field samples. *Environ Microbiol.* 2016;18(5):1403-14.
44. Quince C, Lanzen A, Davenport RJ, Turnbaugh PJ. Removing Noise From Pyrosequenced Amplicons. *Bmc Bioinformatics.* 2011;12.
45. Walters W, Hyde ER, Berg-Lyons D, Ackermann G, Humphrey G, Parada A, et al. Improved Bacterial 16S rRNA Gene (V4 and V4-5) and Fungal Internal Transcribed Spacer Marker Gene Primers for Microbial Community Surveys. *Msystems.* 2016;1(1).
46. Bolyen E, Rideout JR, Dillon MR, Bokulich NA, Abnet CC, Al-Ghalith GA, et al. Reproducible, interactive, scalable and extensible microbiome data science using QIIME 2. *Nat Biotechnol.* 2019;37(8):852-7.
47. Estaki M, Jiang L, Bokulich NA, McDonald D, Gonzalez A, Kosciolek T, et al. QIIME 2 Enables Comprehensive End-to-End Analysis of Diverse Microbiome Data and Comparative Studies with Publicly Available Data. *Curr Protoc Bioinformatics.* 2020;70(1):e100.
48. Callahan BJ, McMurdie PJ, Rosen MJ, Han AW, Johnson AJ, Holmes SP. DADA2: High-resolution sample inference from Illumina amplicon data. *Nat Methods.* 2016;13(7):581-3.
49. Yilmaz P, Parfrey LW, Yarza P, Gerken J, Pruesse E, Quast C, et al. The SILVA and "All-species Living Tree Project (LTP)" taxonomic frameworks. *Nucleic Acids Research.* 2014;42(D1):D643-D8.
50. Caporaso JG, Kuczynski J, Stombaugh J, Bittinger K, Bushman FD, Costello EK, et al. QIIME allows analysis of high-throughput community sequencing data. *Nat Methods.* 2010;7(5):335-6.
51. Huang Y, Li W, Su ZY, Kong AN. The complexity of the Nrf2 pathway: beyond the antioxidant response. *J Nutr Biochem.* 2015;26(12):1401-13.

52. Zhang DD. Mechanistic studies of the Nrf2-Keap1 signaling pathway. *Drug Metab Rev.* 2006;38(4):769-89.
53. Taguchi K, Yamamoto M. The KEAP1-NRF2 System in Cancer. *Front Oncol.* 2017;7:85.
54. Mitsuishi Y, Motohashi H, Yamamoto M. The Keap1-Nrf2 system in cancers: stress response and anabolic metabolism. *Front Oncol.* 2012;2:200.
55. Osburn WO, Kensler TW. Nrf2 signaling: an adaptive response pathway for protection against environmental toxic insults. *Mutat Res.* 2008;659(1-2):31-9.
56. Mariat D, Firmesse O, Levenez F, Guimaraes V, Sokol H, Dore J, et al. The Firmicutes/Bacteroidetes ratio of the human microbiota changes with age. *BMC Microbiol.* 2009;9:123.
57. Koliada A, Syzenko G, Moseiko V, Budovska L, Puchkov K, Perederiy V, et al. Association between body mass index and Firmicutes/Bacteroidetes ratio in an adult Ukrainian population. *BMC Microbiol.* 2017;17(1):120.
58. Stojanov S, Berlec A, Strukelj B. The Influence of Probiotics on the Firmicutes/Bacteroidetes Ratio in the Treatment of Obesity and Inflammatory Bowel disease. *Microorganisms.* 2020;8(11).
59. Martinez I, Lattimer JM, Hubach KL, Case JA, Yang JY, Weber CG, et al. Gut microbiome composition is linked to whole grain-induced immunological improvements. *Isme J.* 2013;7(2):269-80.
60. Kovacs A, Ben-Jacob N, Tayem H, Halperin E, Iraqi FA, Gophna U. Genotype Is a Stronger Determinant than Sex of the Mouse Gut Microbiota. *Microb Ecol.* 2011;61(2):423-8.
61. Ritchie NJ, Schutter ME, Dick RP, Myrold DD. Use of length heterogeneity PCR and fatty acid methyl ester profiles to characterize microbial communities in soil. *Appl Environ Microbiol.* 2000;66(4):1668-75.
62. Albert EJ, Sommerfeld K, Gophna S, Marshall JS, Gophna U. The gut microbiota of toll-like receptor 2-deficient mice exhibits lineage-specific modifications. *Environ Microbiol Rep.* 2009;1(1):65-70.
63. La Reau AJ, Suen G. The Ruminococci: key symbionts of the gut ecosystem. *J Microbiol.* 2018;56(3):199-208.
64. Rainey FA, Janssen PH. Phylogenetic analysis by 16S ribosomal DNA sequence comparison reveals two unrelated groups of species within the genus Ruminococcus. *FEMS Microbiol Lett.* 1995;129(1):69-73.
65. Qin J, Li R, Raes J, Arumugam M, Burgdorf KS, Manichanh C, et al. A human gut microbial gene catalogue established by metagenomic sequencing. *Nature.* 2010;464(7285):59-65.
66. Leschine SB. Cellulose degradation in anaerobic environments. *Annu Rev Microbiol.* 1995;49:399-426.
67. Flint HJ, Bayer EA, Rincon MT, Lamed R, White BA. Polysaccharide utilization by gut bacteria: potential for new insights from genomic analysis. *Nat Rev Microbiol.* 2008;6(2):121-31.
68. Lyra A, Krogius-Kurikka L, Nikkila J, Malinen E, Kajander K, Kurikka K, et al. Effect of a multispecies probiotic supplement on quantity of irritable bowel syndrome-related intestinal microbial phylotypes. *BMC Gastroenterol.* 2010;10:110.
69. Hall AB, Yassour M, Sauk J, Garner A, Jiang X, Arthur T, et al. A novel Ruminococcus gnavus clade enriched in inflammatory bowel disease patients. *Genome Med.* 2017;9(1):103.
70. Henke MT, Kenny DJ, Cassilly CD, Vlamakis H, Xavier RJ, Clardy J. Ruminococcus gnavus, a member of the human gut microbiome associated with Crohn's disease, produces an inflammatory polysaccharide. *Proc Natl Acad Sci U S A.* 2019;116(26):12672-7.
71. Chua HH, Chou HC, Tung YL, Chiang BL, Liao CC, Liu HH, et al. Intestinal Dysbiosis Featuring Abundance of Ruminococcus gnavus Associates With Allergic Diseases in Infants. *Gastroenterology.* 2018;154(1):154-67.
72. Johnson EL, Heaver SL, Walters WA, Ley RE. Microbiome and metabolic disease: revisiting the bacterial phylum Bacteroidetes. *J Mol Med (Berl).* 2017;95(1):1-8.
73. Couturier-Maillard A, Secher T, Rehman A, Normand S, De Arcangelis A, Haesler R, et al. NOD2-mediated dysbiosis predisposes mice to transmissible colitis and colorectal cancer. *J Clin Invest.* 2013;123(2):700-11.

74. Carmichael WW. Cyanobacteria secondary metabolites--the cyanotoxins. *J Appl Bacteriol.* 1992;72(6):445-59.
75. Carmichael WW. The toxins of cyanobacteria. *Sci Am.* 1994;270(1):78-86.
76. Hildebrand F, Nguyen TL, Brinkman B, Yunta RG, Cauwe B, Vandenabeele P, et al. Inflammation-associated enterotypes, host genotype, cage and inter-individual effects drive gut microbiota variation in common laboratory mice. *Genome Biol.* 2013;14(1):R4.
77. Roopchand DE, Carmody RN, Kuhn P, Moskal K, Rojas-Silva P, Turnbaugh PJ, et al. Dietary Polyphenols Promote Growth of the Gut Bacterium *Akkermansia muciniphila* and Attenuate High-Fat Diet-Induced Metabolic Syndrome. *Diabetes.* 2015;64(8):2847-58.
78. Zhang L, Carmody RN, Kalariya HM, Duran RM, Moskal K, Poulev A, et al. Grape proanthocyanidin-induced intestinal bloom of *Akkermansia muciniphila* is dependent on its baseline abundance and precedes activation of host genes related to metabolic health. *J Nutr Biochem.* 2018;56:142-51.
79. Turnbaugh PJ, Ridaura VK, Faith JJ, Rey FE, Knight R, Gordon JI. The effect of diet on the human gut microbiome: a metagenomic analysis in humanized gnotobiotic mice. *Sci Transl Med.* 2009;1(6):6ra14.
80. Lundberg R, Toft MF, August B, Hansen AK, Hansen CH. Antibiotic-treated versus germ-free rodents for microbiota transplantation studies. *Gut Microbes.* 2016;7(1):68-74.

Experiment 1:

Group1: Nrf2^{-/-}, AIN93M (N=9)

Group2: Nrf2^{-/-}, PEITC (N=9)

Experiment 2:

Group3: WT, AIN93M (N=5)

Group4: WT, PEITC (N=5)

Experiment 3:

Group5: WT, AIN93M (N=5)

Group6: WT, AIN93M, DSS (N=5)

Group7: WT, Cranberry, DSS (N=5)

Group8: WT, PEITC, DSS (N=5)

Group9: Nrf2^{-/-}, AIN93M (N=5)

Group10: Nrf2^{-/-}, AIN93M, DSS (N=5)

Group11: Nrf2^{-/-}, Cranberry, DSS (N=5)

Group12: Nrf2^{-/-}, PEITC, DSS (N=5)

AIN93M : Groups 1, 3, 5, 6, 9 and 10

**AIN93M:
Groups 2, 4,
7, 8, 11 and 12**

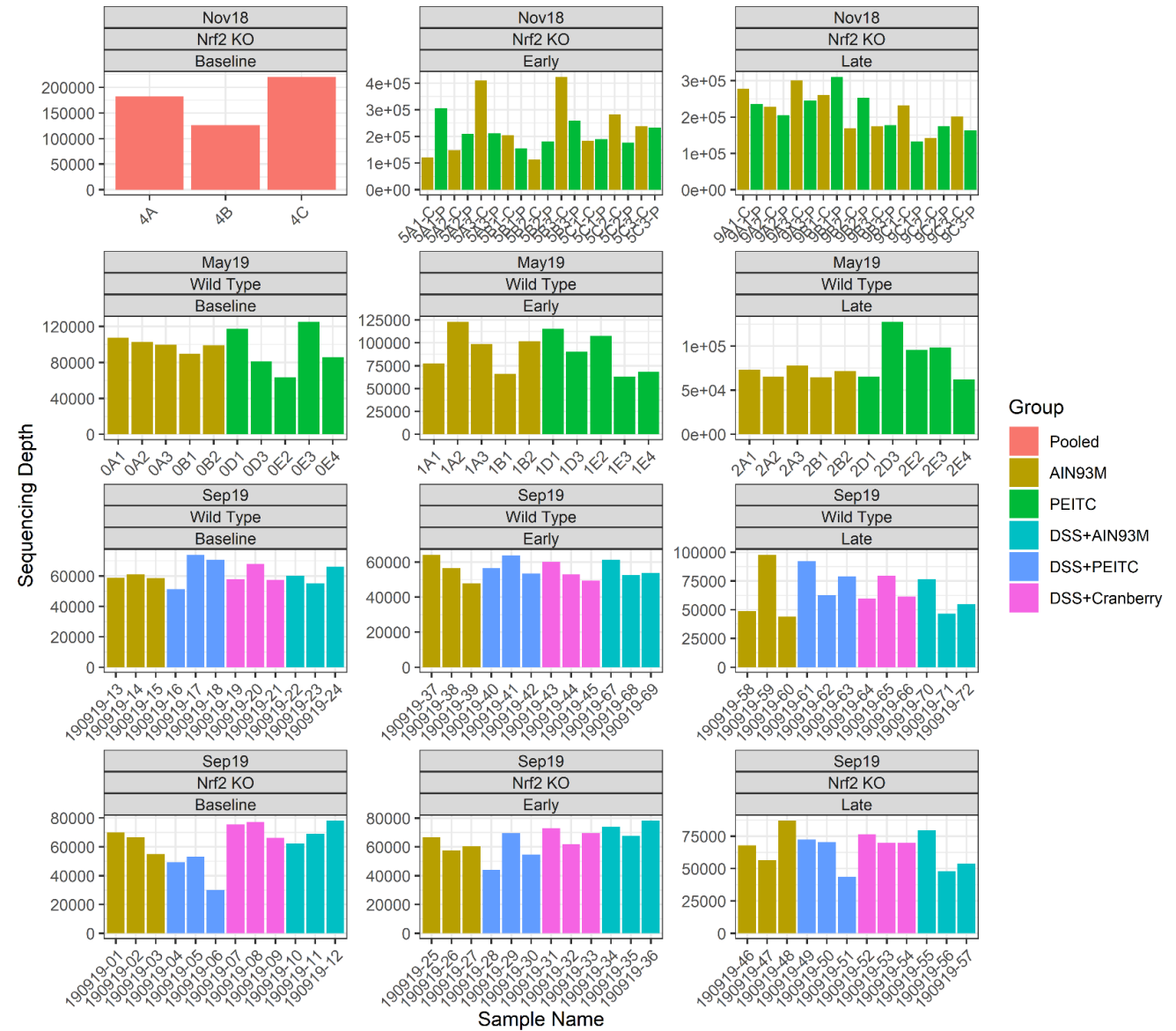
**AIN93M + 0.05% PEITC Groups 2, 4, 8 and 12
AIN93M + Cranberry: Groups 7 and 11**

X X X X X X X X

Week 0 1 2 4 5 6 8

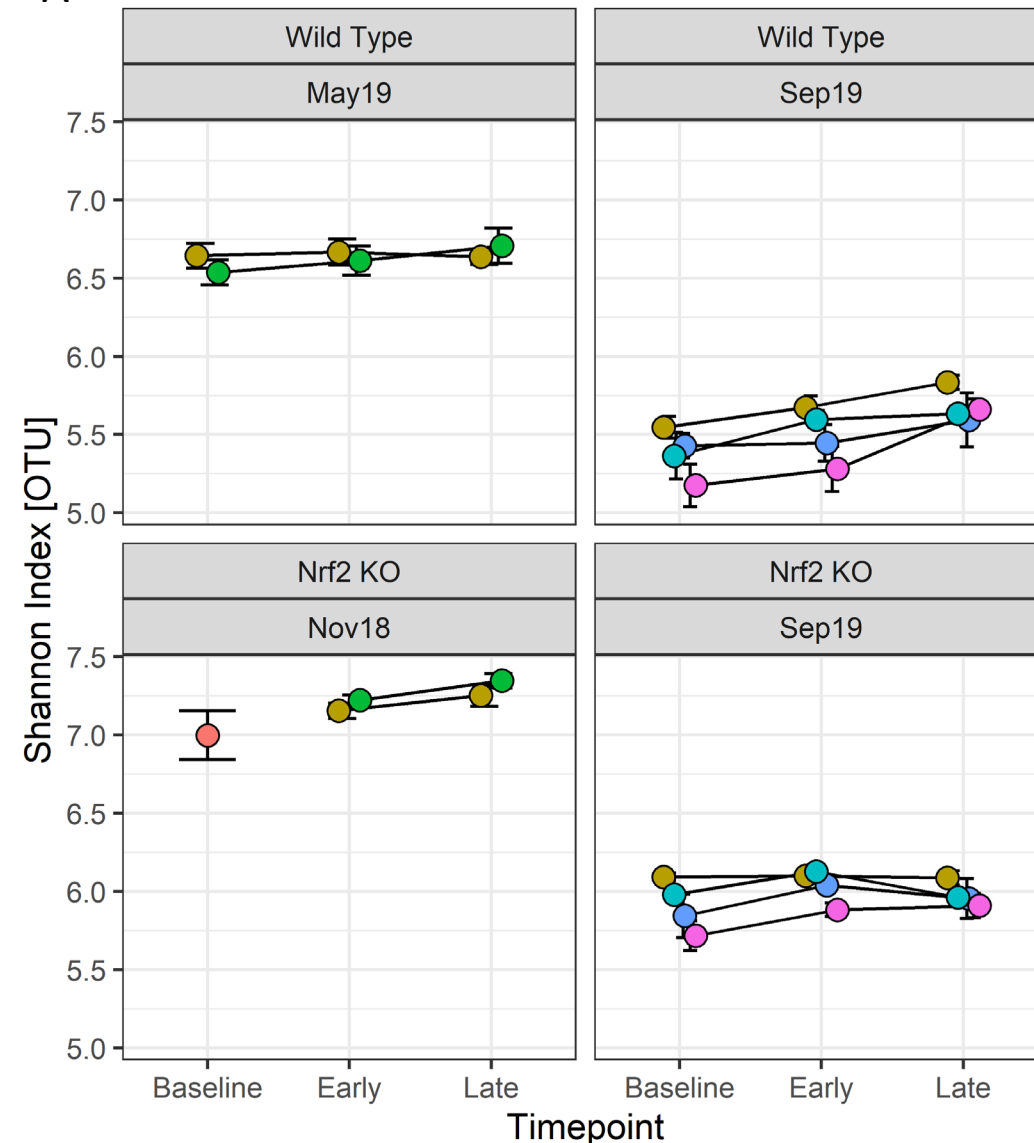
**Gut microbiota
equalization period
(2 weeks)**

Figure 1: Experimental design. Mice fecal samples for the 16S sequencing were collected individually at 3 timepoints – at the end of the 2-week equalization period (Week 0), at an early timepoint (Week 1) and at a late timepoint (Week 4 or Week 8). Samples used for metabolite analysis were collected at an early and a late timepoints (Weeks 2 and Week 6 respectively).



Supplemental Figure 1: 16S sequencing depth (total number of hits per sample).

A



B

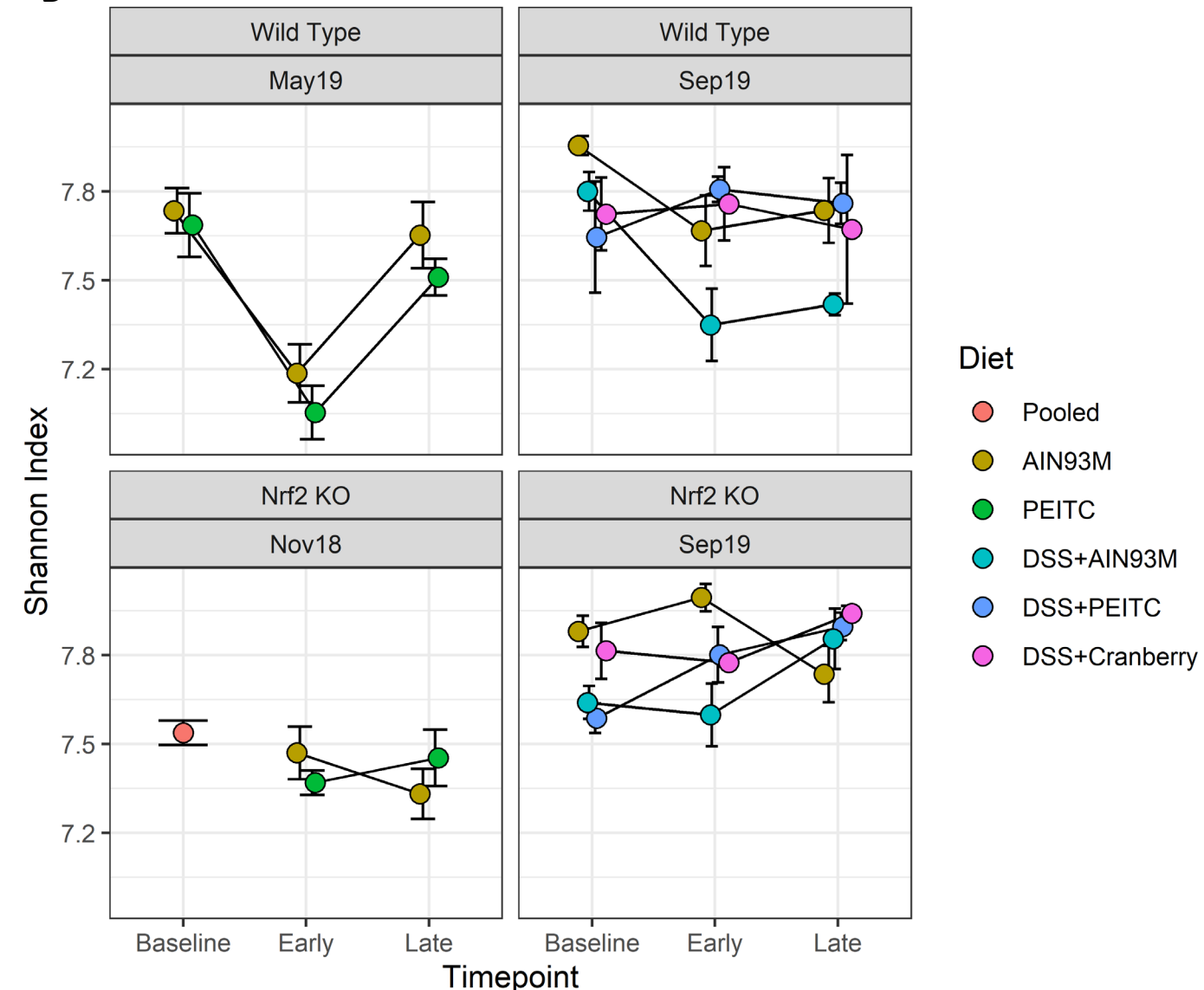
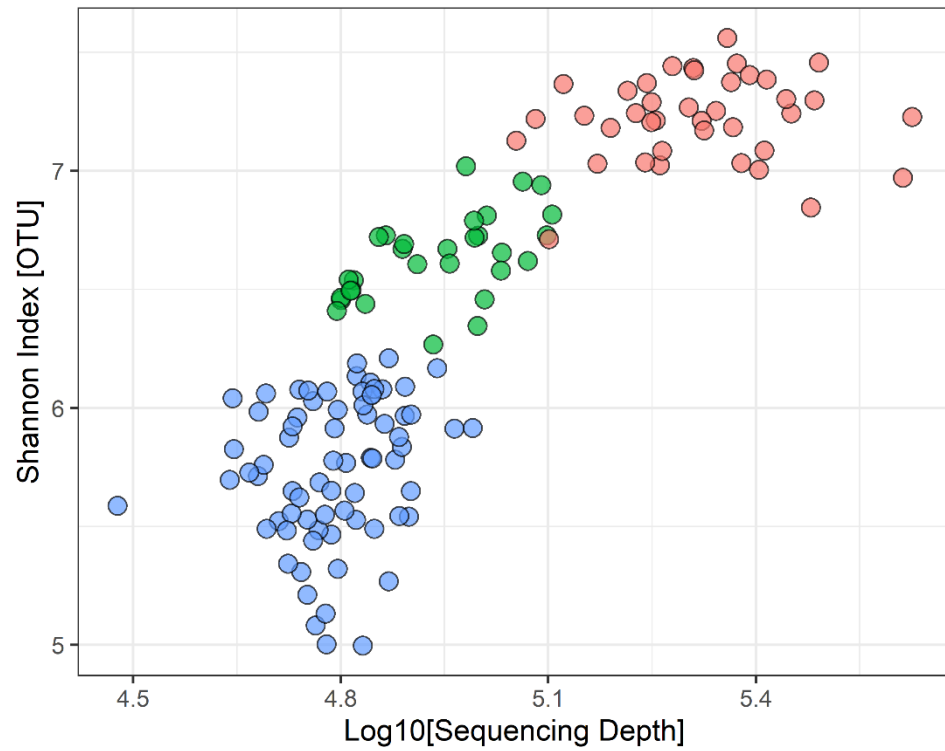
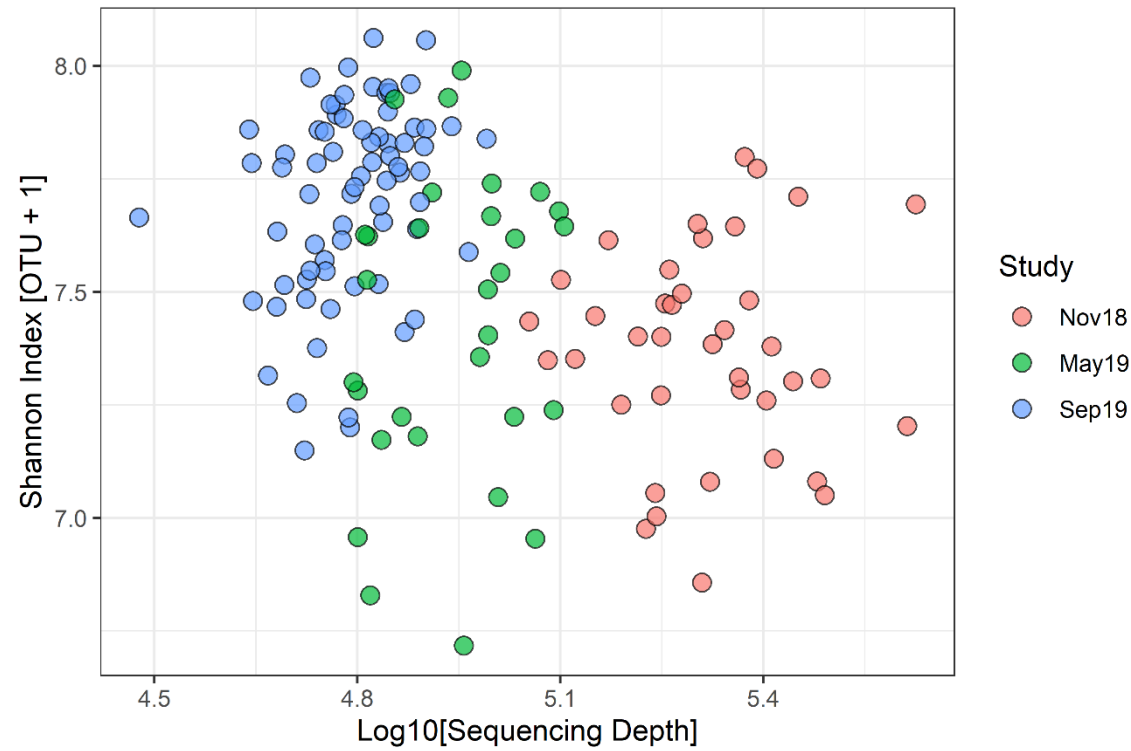
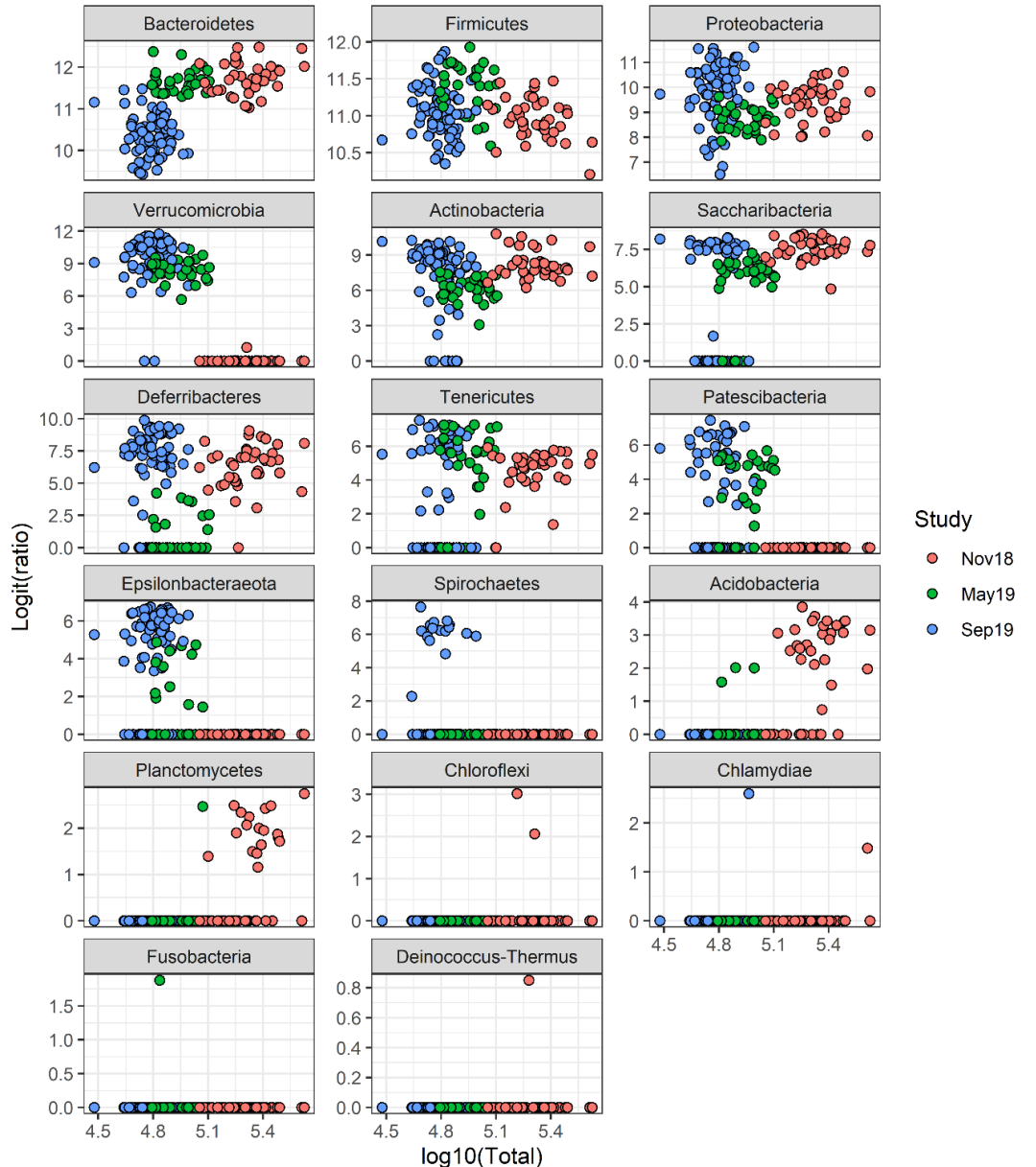


Figure 2: Alpha diversity measured by Shannon index. (A) Averages of Shannon indices calculated on raw OTU numbers and (B) on corrected OTU numbers (OTU+1).

A**B****Study**

- Nov18
- May19
- Sep19

Supplemental Figure 2: Shannon index vs. sequencing depth.



Supplemental Figure 3: logit of the relative abundance of Phylum vs. sequencing depth

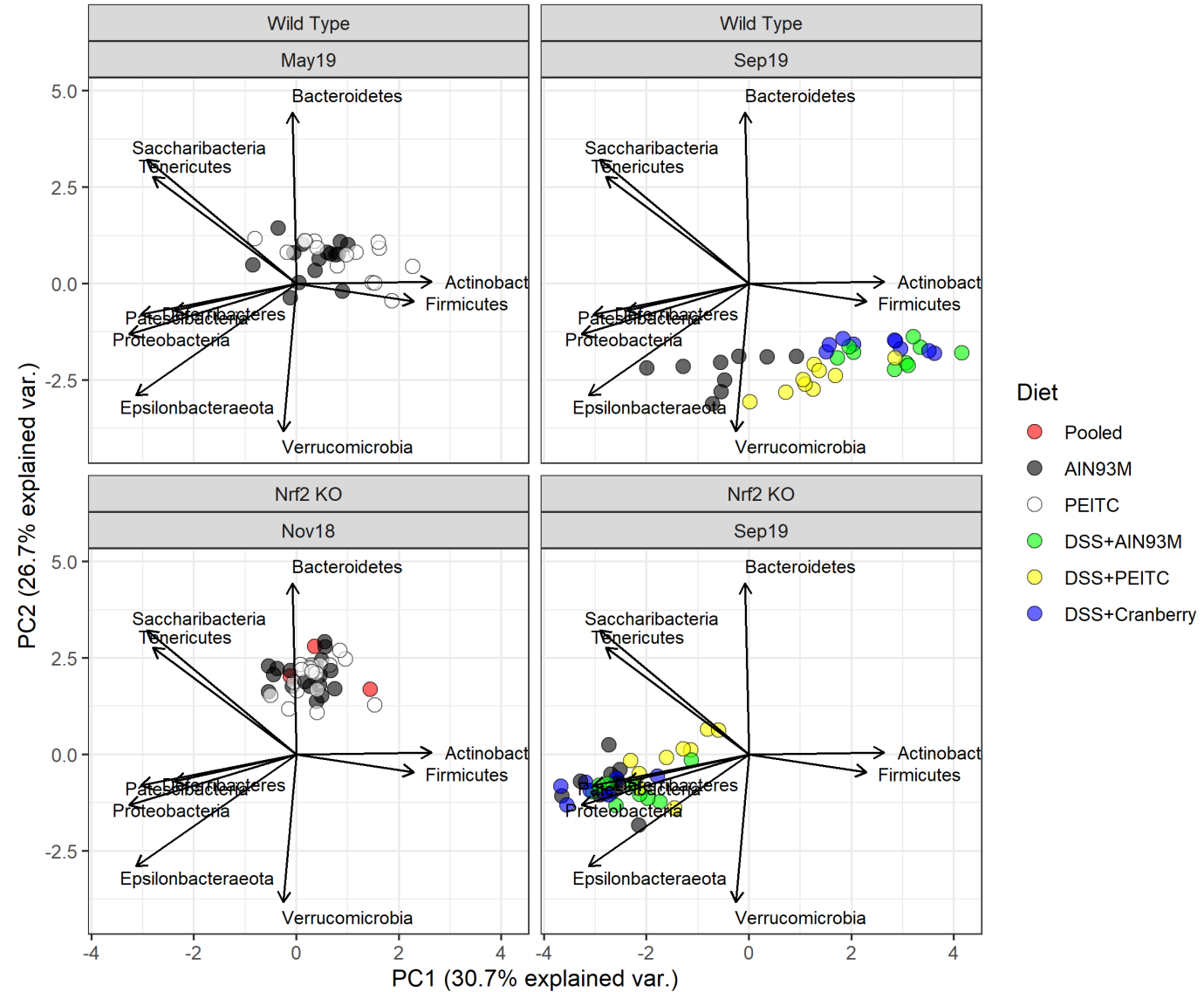


Figure 4: Biplot of logit relative abundance of Phylum

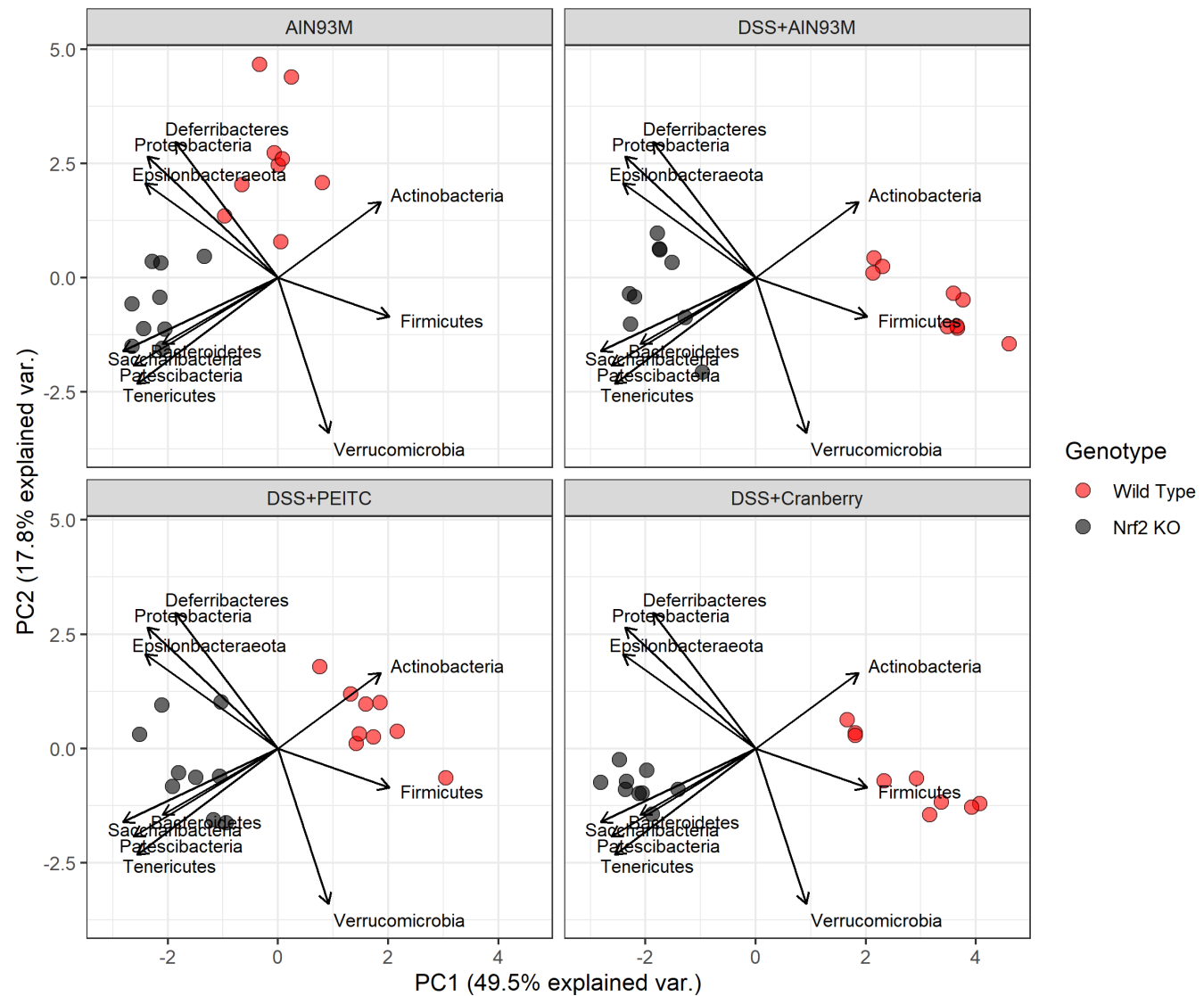


Figure 5: biplot of logit relative abundance of Phylum in Exp03 only

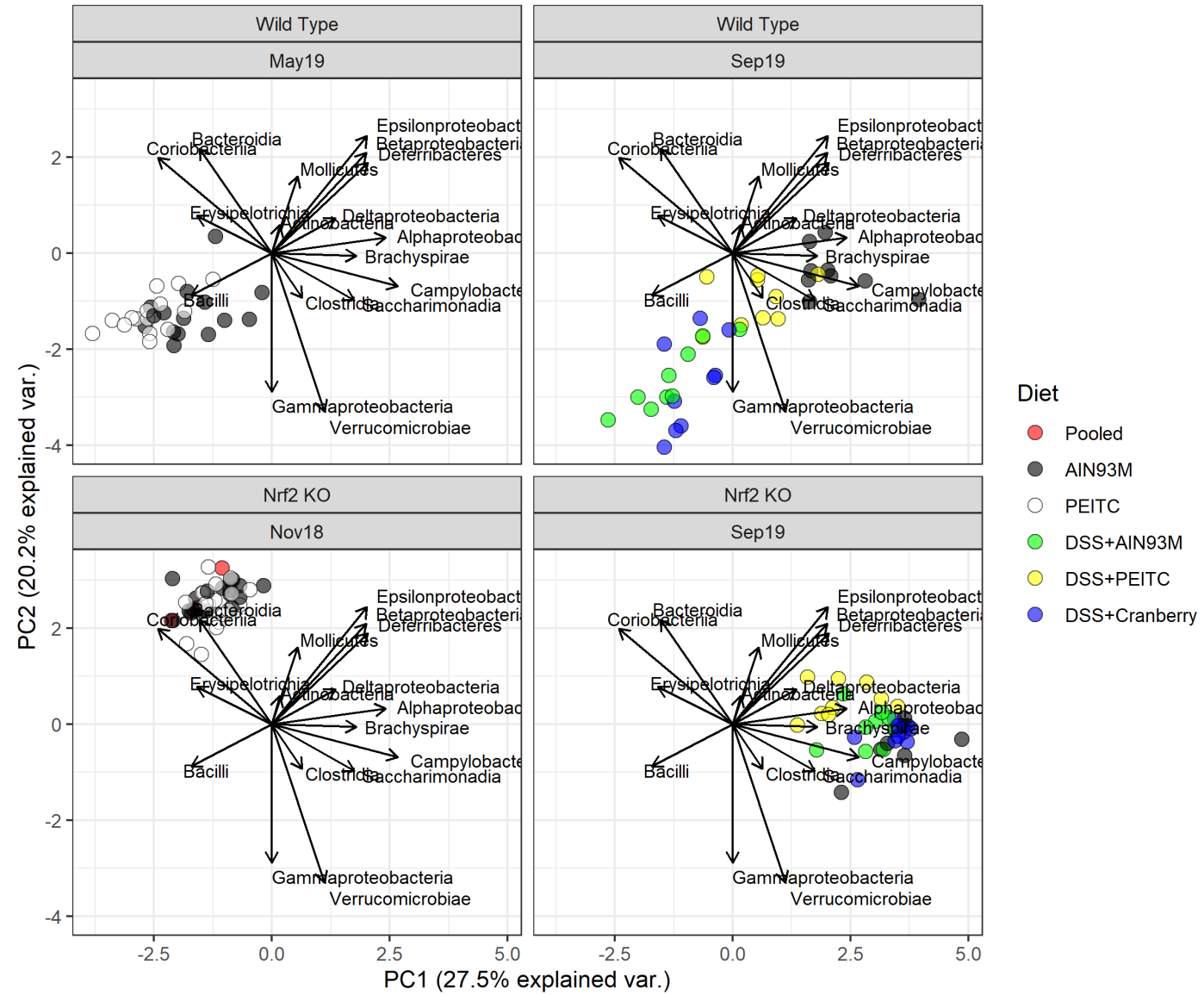


Figure 6: Biplot of logit relative abundance of Classes

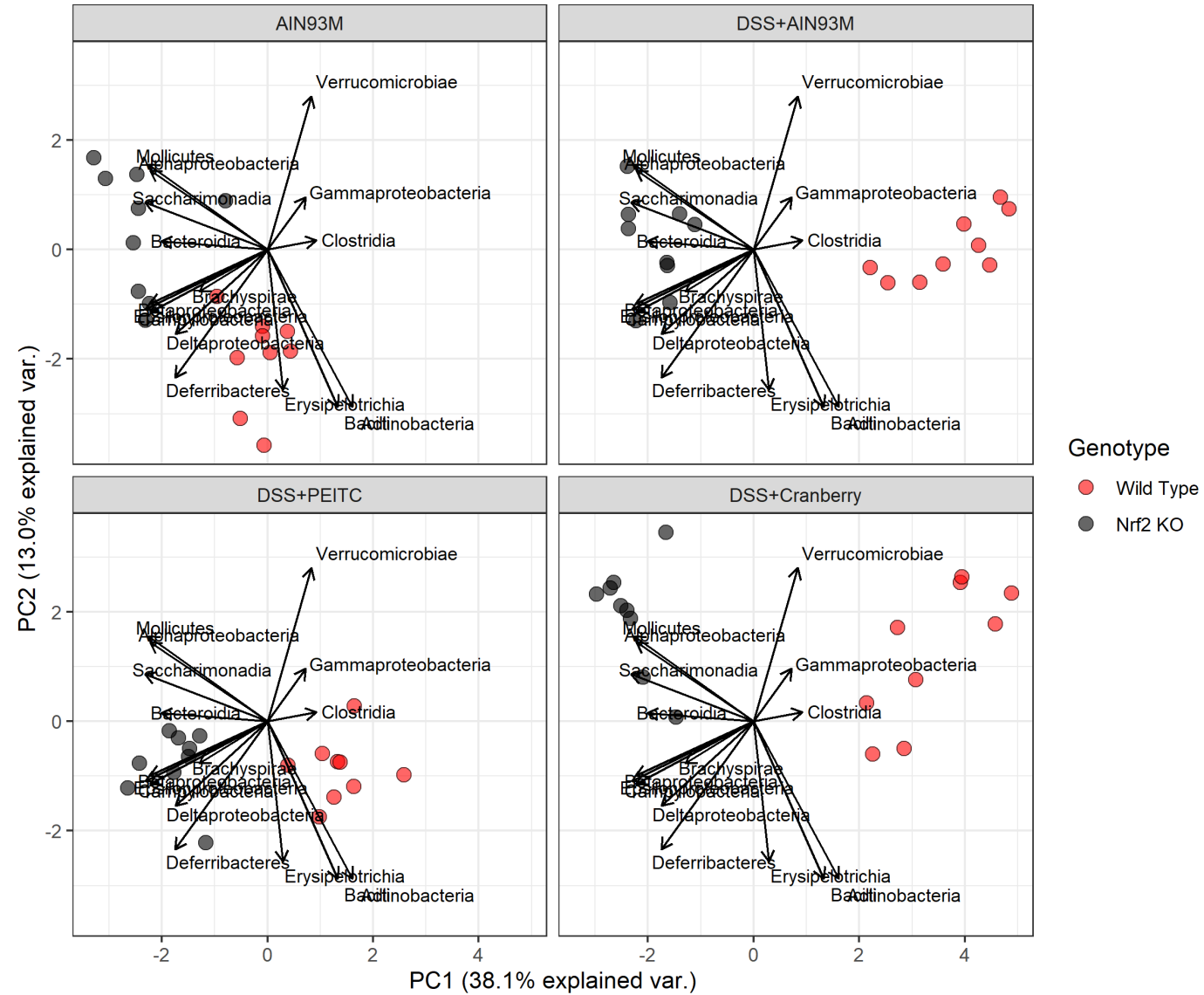


Figure 7: biplot of logit relative abundance of Classes in Exp03 only

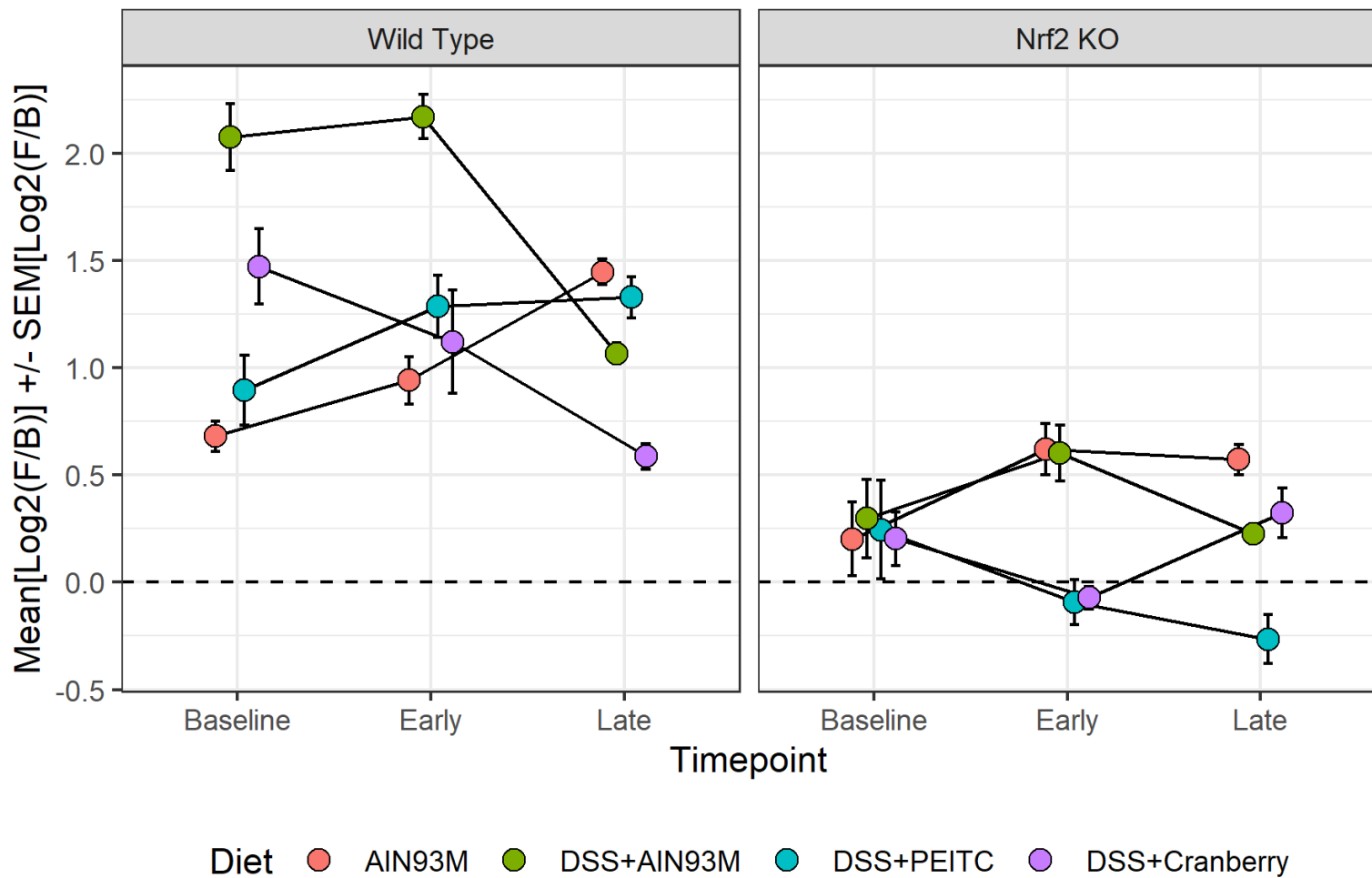


Figure 8: Means of $\log_2 F/B$ ratios by genotype and diet over time. The bars represent standard errors of $\log_2(F/B)$ ratios.

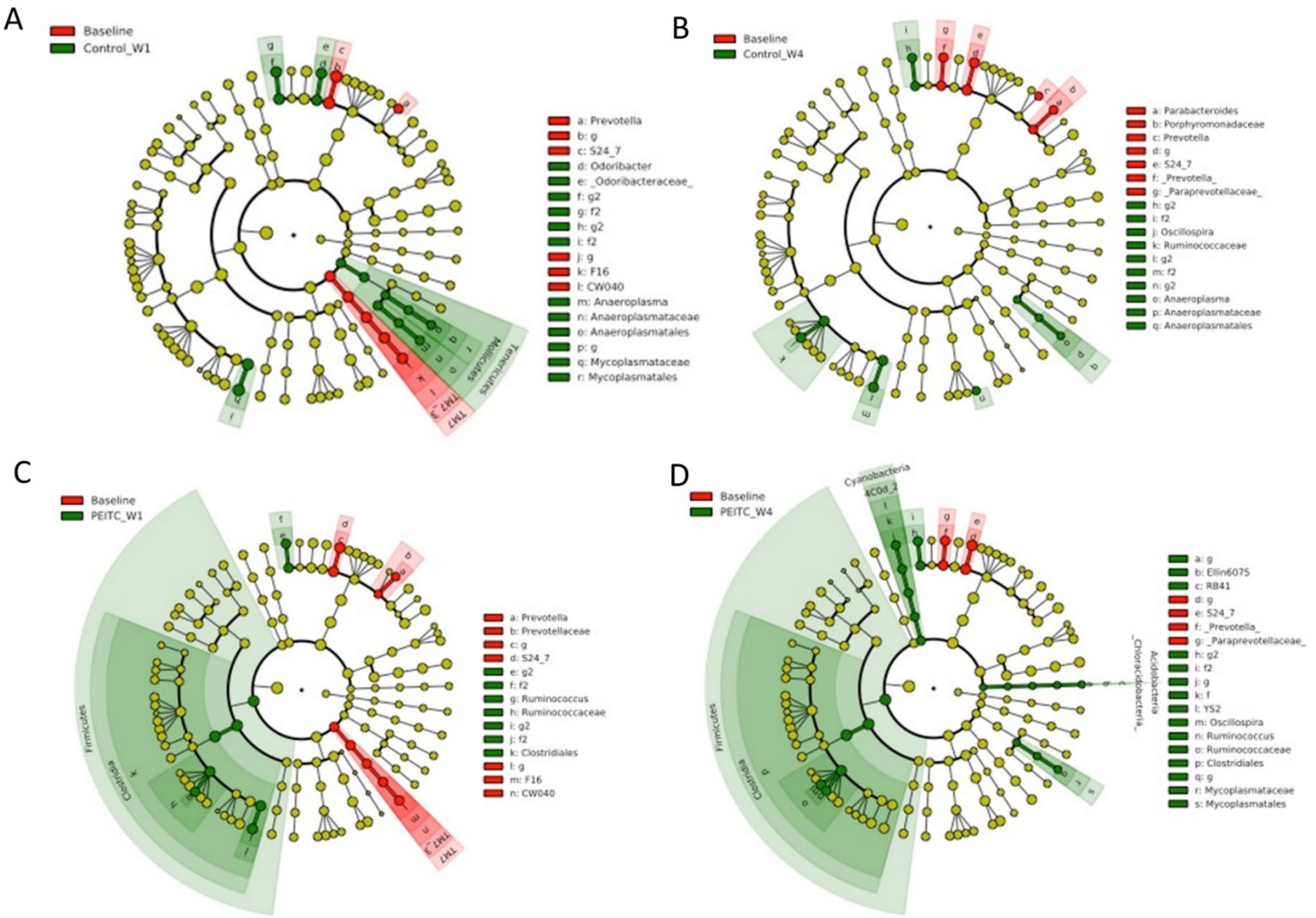


Figure 9: Linear discriminant analysis Effect Size (LEfSe) analysis of aging effect.

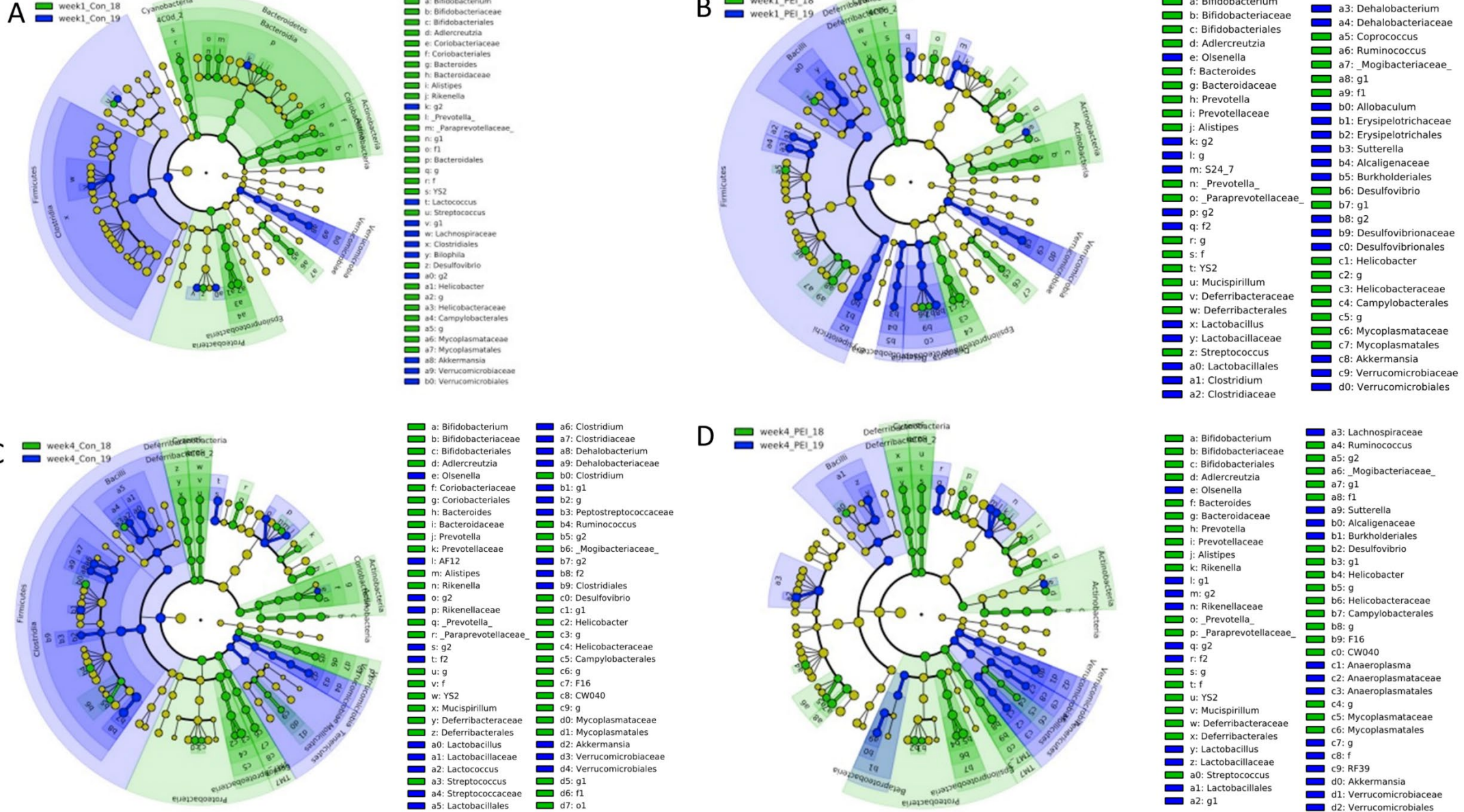
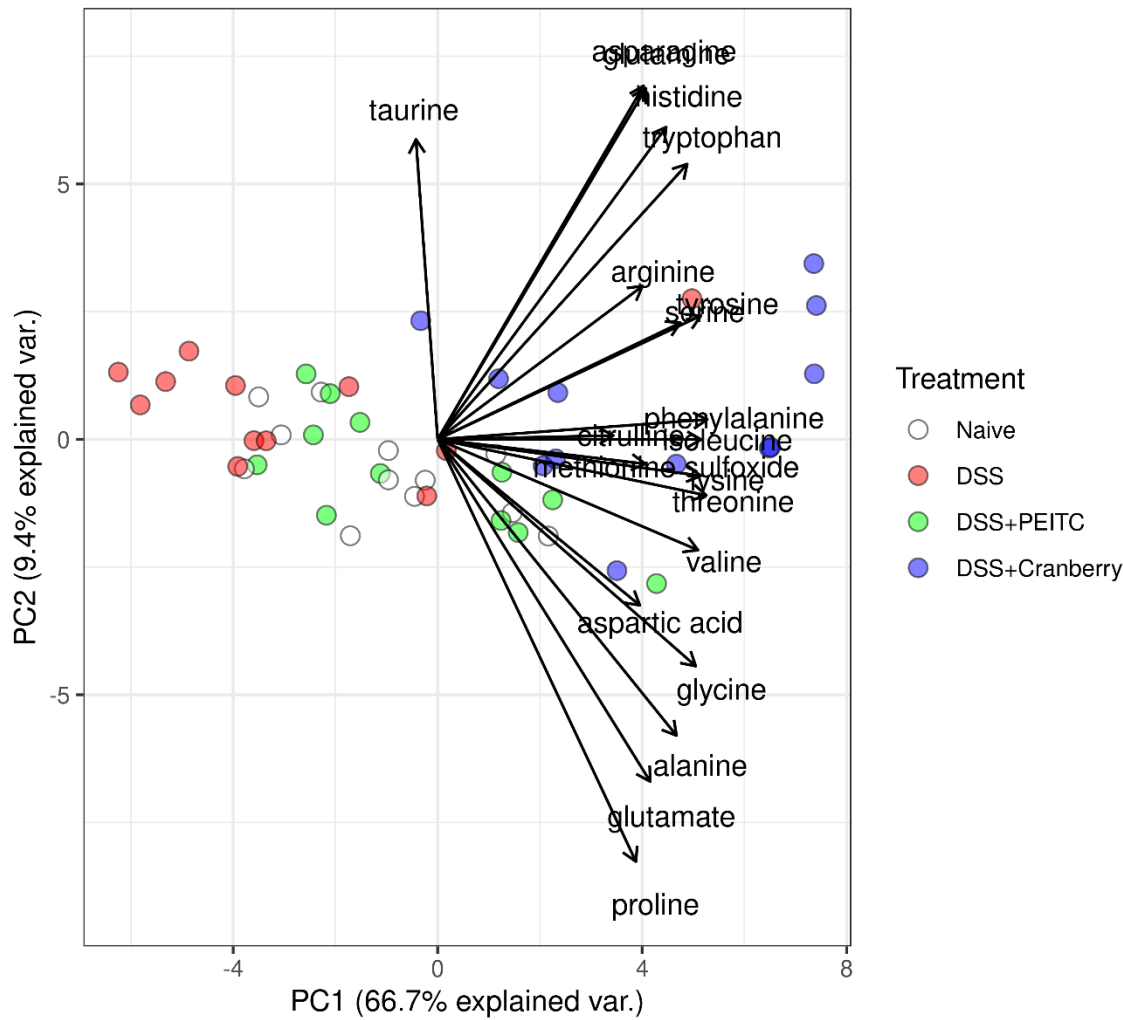


Figure 10: Linear discriminant analysis Effect Size (LEfSe) analysis of diet effect.

A

Biplot of Aminoacids



B

Biplot of Bile Acids

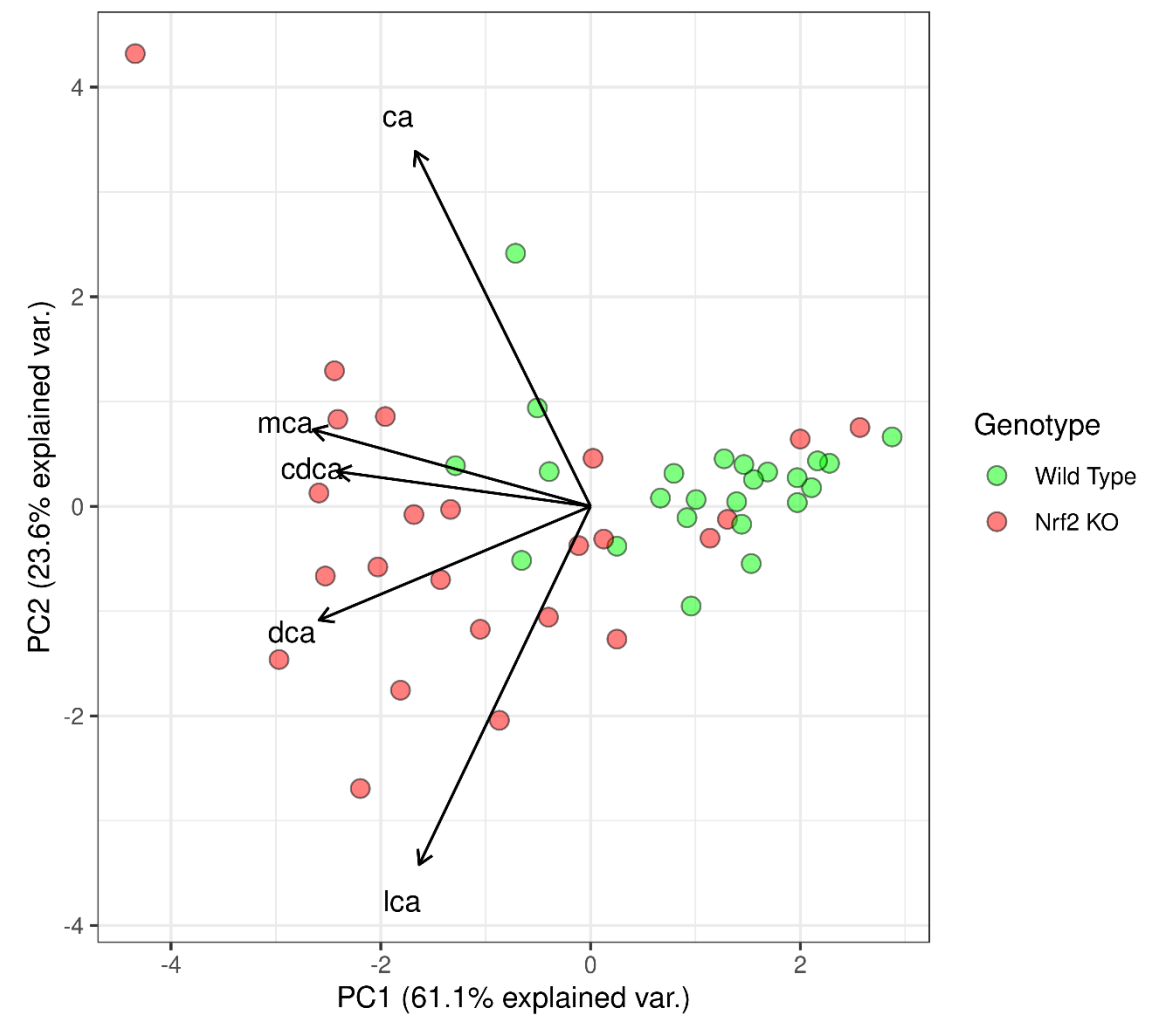


Figure 11: Biplots of amino acids by diet (A) and bile acids by genotype (B) .

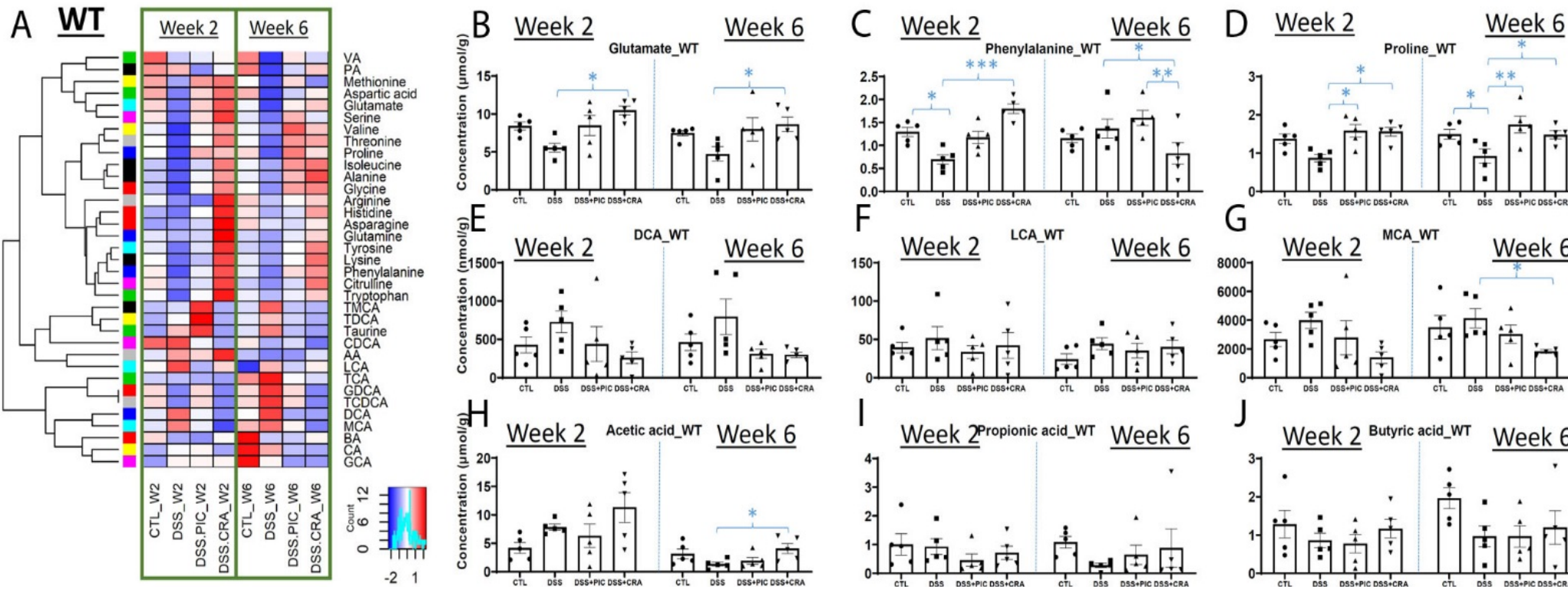


Figure 12: Effects of DSS, PEITC and cranberry cotreatments on fecal metabolome of WT mice. Fecal samples collected at week 2 and 6 of 4 treatments, including control (CTL), DSS, DSS+PEITC (DSS+PIC), and DSS+cranberry (DSS+CRA), were analyzed by 4 LC-MS methods (143). The concentrations of amino acids, bile acids, and SCFA were quantified. (A) A heatmap on the distribution of amino acids, bile acids and SCFA in fecal samples from 4 treatments. (B-D) Concentrations of major amino acids, including glutamate, phenylalanine, and proline. (E-G) Concentrations of major bile acids, including DCA, LCA, and MCA. (H-J) Concentrations of major SCFA, including acetic acid (AA), propionic acid (PA), and butyric acid (BA).

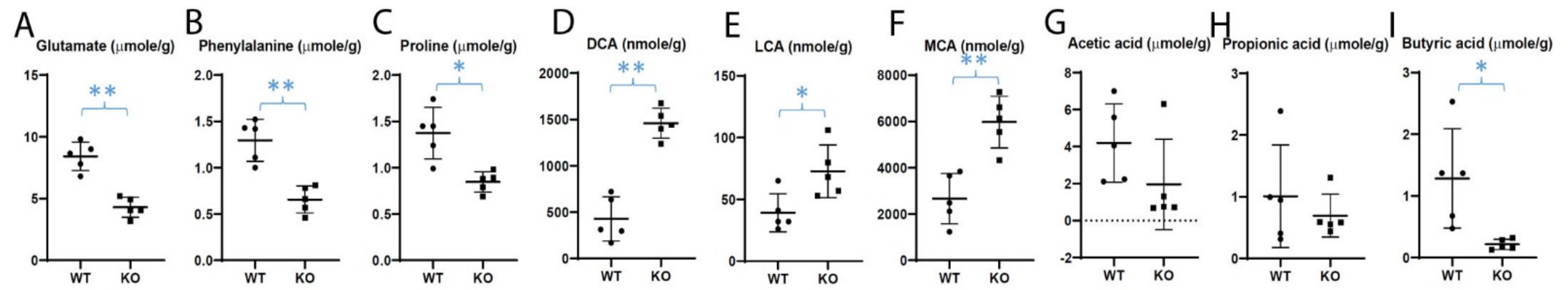


Figure 13: Differences in fecal metabolite profile between WT and Nrf2-null (KO) mice. The concentrations of amino acids, bile acids, and SCFA were quantified in the fecal samples from untreated WT and KO mice (143). (A-C) Concentrations of glutamate, phenylalanine, and proline. (D-F) Concentrations of major bile acids. (G-I) Concentrations of major SCFA.

| Forward Primer | Reverse Primer |
|------------------------|----------------------|
| 515F (Parada) | 806R (Apprill) |
| GTG YCAG CMGCC GCGGTAA | GGACTACNVGGGTWTCTAAT |

Supplemental Table 1: V4 primer sequence used for 16s RNA sequencing library preparation

| Kingdom | Experiment 1: Nrf2 KO Mice | Experiment 2: WT Mice | Experiment 3: WT and Nrf2 KO | Combined |
|-----------|-------------------------------|--------------------------|---------------------------------|-----------------|
| Bacteria | 10,197 (94.78%) | 7,994 (98.34%) | 7,558 (96.07%) | 22,251 (95.73%) |
| Eukaryota | 472 (4.39%) | 116 (1.43%) | 232 (2.95%) | 812 (3.49%) |
| Archaea | 4 (0.04%) | 0 (0%) | 2 (0.03%) | 6 (0.03%) |
| Unknown | 86 (0.80%) | 19 (0.23%) | 75 (0.95%) | 175 (0.75%) |

Table 1: OTUs mapping to Kingdoms. Number of OTU (% total)

| Predicted treatment/diet PC1+PC2+PC3 | Actual treatment/diet | | | |
|---|-----------------------|-------|-------------|-----------------|
| | DSS | Naïve | DSS + PEITC | DSS + Cranberry |
| DSS | 8 | 4 | 4 | 0 |
| Naïve | 2 | 4 | 1 | 0 |
| DSS + PEITC | 1 | 3 | 6 | 1 |
| DSS + Cranberry | 1 | 1 | 1 | 11 |

Table 2: multinomial regression predictions of treatment groups by microbial metabolite PCA

| Predicted genotype | Actual genotype | |
|--------------------|-----------------|---------|
| | Wild Type | Nrf2 KO |
| Wild Type | 18 | 6 |
| Nrf2 KO | 8 | 16 |

Table 3: multinomial regression predictions of genotype by microbial metabolite PCA